

RESEARCH ARTICLE

The effects of land use change on land surface temperatures and its health risks on street traders in Bulawayo, Zimbabwe

Shelton Mthunzi Sithole^{1*}, Walter Musakwa², James Magidi³

1 Department of Urban and Regional Planning, University of Johannesburg, Cnr Siemert & Beit Streets, Johannesburg, South Africa, **2** Department of Geography, Environmental Management & Energy Studies, Faculty of Science, University of Johannesburg, Johannesburg, South Africa, **3** Geomatics Department, Tshwane University of Technology, Pretoria, Gauteng, South Africa

* rmthunzishelton@gmail.com



OPEN ACCESS

Citation: Sithole SM, Musakwa W, Magidi J (2026) The effects of land use change on land surface temperatures and its health risks on street traders in Bulawayo, Zimbabwe. *PLOS Clim* 5(1): e0000716. <https://doi.org/10.1371/journal.pclm.0000716>

Editor: Oscar Brousse, University College London The Bartlett Faculty of the Built Environment, UNITED KINGDOM OF GREAT BRITAIN AND NORTHERN IRELAND

Received: December 3, 2024

Accepted: December 1, 2025

Published: January 5, 2026

Copyright: © 2026 Sithole et al. This is an open access article distributed under the terms of the [Creative Commons Attribution License](https://creativecommons.org/licenses/by/4.0/), which permits unrestricted use, distribution, and reproduction in any medium, provided the original author and source are credited.

Data availability statement: The authors confirm that the data supporting the findings of this study are available within the article.

Funding: The author(s) received no specific funding for this work.

Abstract

Rapid urbanization and land use change in African cities are intensifying the urban heat island effect, yet their specific human health consequences for vulnerable populations remain critically understudied. This research addresses this gap by investigating the nexus between land surface temperature (LST) rise and health risks for street traders in Bulawayo, Zimbabwe, a city experiencing significant urban expansion. We integrated multi-temporal Landsat and MODIS satellite data (1995–2022) with socio-economic surveys of 150 street traders to quantify thermal trends and their perceived health impacts. Our analysis reveals a significant 228% increase in built-up area, driving a pronounced warming trend, with summer LST reaching 43.4°C. This thermal amplification is strongly correlated with impervious surfaces and shows a clear inverse relationship with vegetation cover. Critically, survey data expose severe heat-related morbidity, with nearly all traders (98.7%) reporting symptoms like headaches and 63.3% experiencing fainting spells, with the highest burden concentrated in high-density and industrial zones. This study conclusively demonstrates that land use changes are directly translating into severe occupational health hazards for the informal workforce. The findings provide an urgent, evidence-based mandate for urban planners and public health officials to implement targeted interventions—such as strategic urban greening, provision of shade infrastructure, and heat early-warning systems—to safeguard vulnerable populations and build climate-resilient cities in the Global South.

1. Introduction

The mushrooming acceleration trend of urbanisation, a global phenomenon, has profound implications for the environment and human health [1]. As built-up areas expand and densify, land-use and land-cover (LULC) changes occur, with significant

Competing interests: The authors have declared that no competing interests exist.

consequences for local and regional climates [2–4]. A significant consequence of urban expansion is the alteration of land surface temperature (LST), leading to the urban heat island (UHI) effect [5]. The subsequent implications of elevated LST for human health are a growing concern within the context of urbanisation [6,7], underscoring an urgent need for global scientific action to study the health burden of climate change [8,9].

Studies reveal that the Earth is now 1.2°C warmer than pre-industrial levels and may warm by 1.5°C as early as 2028 [10]. Excessively high temperatures are projected to cause the annual loss of over 2% of total working hours worldwide, either through heat exposure or reduced workplace productivity [11]. In Africa, up to 5% of total working hours are expected to be lost [11], with conspicuous impacts on human health [12].

Southern Africa is experiencing significant impacts from climate change [13]. Mean annual temperatures rose between 1.04°C and 1.44°C from 1961 to 2015, and further increases are expected [14]. Over the past 40 years, the region has experienced an increase in hot days and a decline in the frequency of cold extremes [15]. The Special Report on Global Warming of 1.5°C identified the region as a climate change “hotspot,” where impacts are anticipated to be more severe than the global average [9]. [9] emphasises the urgent need for action in Southern Africa, as rising temperatures increase human heat exposure and alter the spread of infectious diseases. The Generalised Systems Moments (GSM) method approach proposed by [16] validates a positive correlation between the size of the informal sector and the susceptibility of African nations to climate change. Research indicates that nations with limited social, economic, or governance-related adaptive capacity are more vulnerable to climate change than those with high adaptive capacity [17,18].

In addition to its effects on public health, heat stress is expected to significantly reduce labour productivity, potentially decreasing global Gross Domestic Product (GDP) by several percentage points [11,19].

Once a thriving industrial hub, Bulawayo has experienced rapid urban growth and development in recent decades [20,21]. This expansion has been accompanied by significant changes in land-use patterns, converting green spaces and agricultural land into built-up areas [20]. Investigating the city’s vulnerability to the urban heat island (UHI) effect—which elevates temperatures across different land-use categories—is therefore essential [22]. As a vital component of the informal economy, street vendors provide affordable goods and services to urban populations [23]. However, they are particularly vulnerable to the adverse effects of climate change and urban heat stress [24], as elevated temperatures can lead to heat-related illnesses, reduced productivity, and economic hardship [24].

Research on urban sprawl, LST, and human health in developed countries is increasing [25], yet a significant gap remains in understanding these interconnected issues in African cities [7]. Most existing literature on Africa treats urban sprawl, LST, and health risks as isolated phenomena, failing to integrate these aspects to examine their collective impact on vulnerable populations, particularly street vendors. While street vendors are an essential part of urban economies in many African cities [24],

their specific challenges and health risks in the context of urban sprawl and rising LST remain underexplored. This oversight is troubling, especially considering that these environmental factors are increasingly linked to climate change, which disproportionately affects marginalised communities.

Thus, the aim of this study is to investigate the urban climate dynamics in Bulawayo, Zimbabwe, with a dual focus. First, the study seeks to characterise the cross-sectional temperature profiles associated with various land-use categories. Second, it aims to examine street vendors' health risks and challenges resulting from elevated land surface temperatures (LST). By integrating spatial temperature analysis with socio-economic assessments, this study seeks to elucidate the interplay between urban heat and public health, particularly in marginalised communities that rely on street vending as a primary source of income.

This study advances multiple Sustainable Development Goals (SDGs). It supports SDG 11 (Sustainable Cities and Communities) by proposing heat mitigation strategies like urban greening, aligns with SDG 3 (Good Health and Well-being) by addressing heat-related illnesses, and contributes to SDG 13 (Climate Action) through the preservation of green spaces. Advocating for safer working conditions furthers SDG 8 (Decent Work and Economic Growth), while promoting inclusive urban planning addresses SDG 10 (Reduced Inequalities). By integrating geospatial and socio-economic data, the research offers a multidisciplinary framework for equitable, climate-resilient development in African cities.

Examining these patterns as scientific evidence is crucial for promoting the creation of climate-resilient and liveable urban areas [26,27]. This research is particularly important for regional and urban spatial planners, as it offers insights into heat-related health risks and provides adaptation and coping strategies for elevated land surface temperatures (LST) and urban heat islands (UHIs). Given that public health threats posed by UHIs—as highlighted by remotely sensed LST data and street vendor perceptions—have received limited attention in the Bulawayo research context, this study aims to address this gap through a groundbreaking analysis. Understanding these dimensions is vital for enhancing the resilience and sustainability of urban environments and is crucial for informing effective policies that safeguard the health and livelihoods of vulnerable populations. Bridging this gap is not merely an academic endeavour but a necessary step toward fostering equitable urban development in Africa. The findings will inform evidence-based policies and urban planning strategies to create more sustainable and resilient urban environments.

2. Study area

Bulawayo, the second-largest city in Zimbabwe, is a testament to urban resilience. Historically the nation's industrial hub, the city has experienced numerous factory closures and out-migration due to a prolonged economic downturn [28]. Despite these challenges, Bulawayo is the first Zimbabwean city to adopt and implement an operative Master Plan and has received consistent accolades for being the best-run municipal authority in the country [20].

The city is situated at an elevation of approximately 1,328 metres above sea level. Its climate is characterised by rainfall from October to March, with an annual average of 600 mm [29]. The mean annual temperature is 25°C, with October being the warmest month (average maximum of 29°C) and July the coolest (average minimum of 9°C; average of 21°C). According to the latest census, Bulawayo's population was estimated to be 665,940 in 2022 [30].

Proximity to the Kalahari Desert makes the city prone to droughts, resulting in chronic water shortages. Consequently, residents experience water shedding for a significant portion of the year [31]. As shown in the study area map (Fig 1), Bulawayo is bounded by longitudes 28.3874°E and 28.6968°E and latitudes 20.2587°S and 19.9615°S.

3. Data and methods

This research utilised a mixed-methods approach that integrated geospatial technology with surveys of street traders to comprehensively understand the complex interactions between land surface conditions, temperature variations, land-use patterns, and trader well-being. This methodology provides a robust evidence base to inform decision-makers in

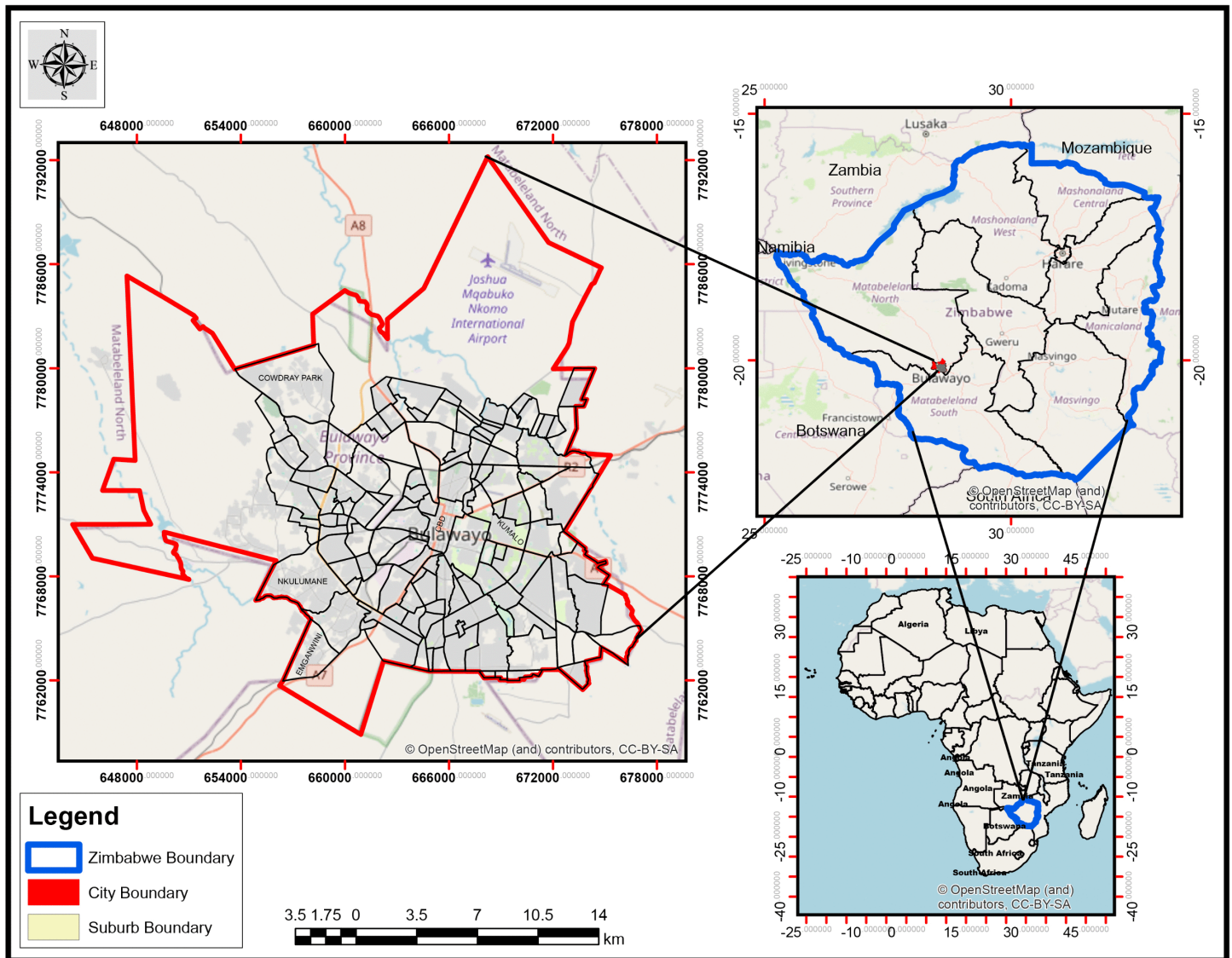


Fig 1. Study area map showing the location of the city of Bulawayo in Zimbabwe.

<https://doi.org/10.1371/journal.pclm.0000716.g001>

developing and implementing policies that support sustainable urban development and enhance the welfare of street traders. The research design is summarised in (Fig 2).

3.1 Ethics statement

The study received ethical clearance from the Ethics and Plagiarism Committee (FEPC) of the Faculty of Engineering and the Built Environment at the University of Johannesburg (ethical clearance number UJ_FEBC_FEPC_01088) and from the City of Bulawayo (reference number MT/LM.74-00-00). Written informed consent was obtained from all participants prior to questionnaire administration. During fieldwork, two minor participants were accompanied by legally authorised guardians (parents). In these cases, consent procedures were adapted to ensure comprehension, with formal documentation provided by the guardians.

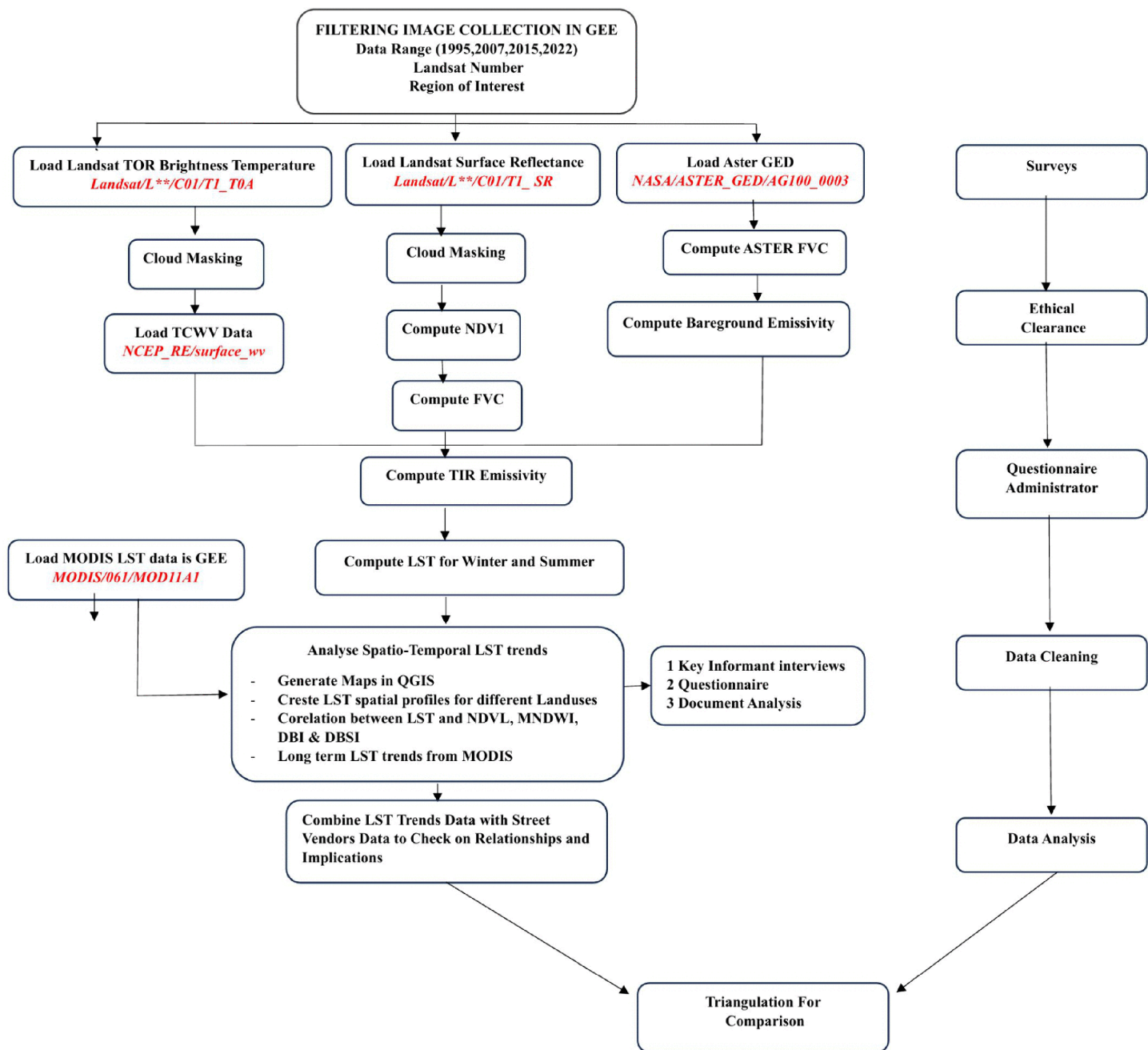


Fig 2. Methodology flow chart applied in this study.

<https://doi.org/10.1371/journal.pclm.0000716.g002>

3.2 Geospatial methodology

This study aimed to investigate changes in summer and winter LST across different land uses for the years 1995, 2007, 2015, and 2022. Landsat imagery, provided by the United States Geological Survey (USGS) and accessed via Google Earth Engine (GEE), a geospatial cloud computing platform was carefully selected to represent both winter (May–July) and summer (October–November) seasons. Landsat data were chosen due to their long-term temporal availability, with

missions dating back to 1972, making them a reliable source for continuous Earth observations. The analysis relied on the Landsat Surface Reflectance Collection 2, Level-2 data for Landsat 5 (Thematic Mapper, TM) and Landsat 8 (Operational Land Imager, OLI) from GEE to estimate LST. The USGS provides pre-processed and calibrated thermal infrared bands for Landsat 4–9 collections within GEE [32]. These data are calibrated and resampled to a 30-meter spatial resolution and are available in different quality tiers [33]. Tier 1 consists of the highest quality scenes, which were used for this time-series analysis of LST in Bulawayo. Lower-quality scenes are accessible from Tier 2 [34].

Additionally, the study utilised near-infrared (NIR), shortwave infrared (SWIR), and visible channels to calculate the Normalised Difference Vegetation Index (NDVI), the Modified Normalised Difference Water Index (MNDWI), the Dry Built-Up Index (DBI), and the Dry Bare-Soil Index (DBSI). The properties of the spectral bands used are described in Table 1.

3.2.1 Moderate resolution imaging spectroradiometer (MODIS) LST and emissivity. Google Earth Engine (GEE) was employed to retrieve land surface temperature (LST) data from the Terra MODIS MOD11A1 Version 6.1 product (2000–2024) at a 1 km resolution to analyse long-term trends in Bulawayo. The dataset provides per-pixel LST values derived from thermal infrared bands [35] using a split-window algorithm, accompanied by quality control flags, emissivity values, and observation metadata. Version 6.1 incorporates key calibration improvements, including corrections for scan-angle effects, optical crosstalk, and updated look-up tables (2012–2017).

This study also utilised Landsat Level 2 Surface Temperature (LST) data derived from the thermal infrared (TIR) bands (Band 6 for Landsat 4–7 and Band 10 for Landsat 8–9) to analyse LST trends in Bulawayo from 1995 to 2022. The Landsat 4–9 LST product, accessed via GEE, was generated through a systematic processing chain applied to Landsat Collection 2 Level 1 data. The workflow incorporated: (1) conversion of raw digital numbers to Top-of-Atmosphere (TOA) reflectance and brightness temperature; (2) atmospheric correction using humidity, geopotential height, elevation, and temperature profiles from the National Aeronautics and Space Administration’s (NASA) Modern-Era Retrospective Analysis for Research and Applications (MERRA-2); (3) emissivity adjustment based on the Advanced Spaceborne Thermal Emission and Reflection Radiometer (ASTER) Global Emissivity Dataset (GED) and ASTER Normalised Difference Vegetation Index (NDVI) to account for surface spectral properties; and (4) LST retrieval via a single-band algorithm, which inverts the Planck function after correcting for atmospheric and emissivity effects [36]. The dataset was validated against ground observations and MODIS LST products to ensure accuracy.

3.2.2 Loading collections in GEE. The acquisition dates were judiciously chosen to select exclusively cloud-free scenes. In cases where completely cloud-free scenes were unavailable, the script employed cloud-masking techniques that utilised the quality assurance (QA) bands to mitigate the impact of cloud cover on the retrieved data. Surface reflectance data was retrieved to compute the Normalised Difference Vegetation Index (NDVI), an essential parameter for estimating both the Fractional Vegetation Cover (FVC) and land surface emissivity [37]. To select images for specific seasons and years within the Bulawayo study area, the analysis specified date ranges, the Landsat satellite platform, an NDVI flag, and the region of interest (ROI). The NDVI flag ensured that the algorithm applied an NDVI-based emissivity

Table 1. Properties of the Landsat Satellite Data used in this study.

Data	Sensor	Bands Used	Resolution	Dates
Landsat 5	TM	Visible- B1,2&3, NIR-B4, SWIR- B5, TIR - B6	30, 30, 30, 120(30)	12/06/1995, 02/10/1995, 13/06/2007, 01/09/2007
Landsat 8	OLI	Visible- B2,3&4, NIR- B5, SWIR- B6, TIR- B10&11	30, 30, 30, 100	19/06/2015, 23/09/2015 08/07/2022, 26/09/2022

<https://doi.org/10.1371/journal.pclm.0000716.t001>

correction. Using these filters, the script was written to retrieve Top of Atmosphere (TOA) brightness temperature data from Landsat 5 and Landsat 8, alongside surface reflectance information [38].

3.2.3 Atmospheric correction. The thermal infrared (TIR) bands of the Landsat series (Band 6 and band 10 for Landsat 4–7 Landsat 8–9 respectively) were atmospherically corrected to account for the influence of atmospheric constituents on surface temperature retrieval. This correction was performed using the Moderate Resolution Atmospheric Transmission (MODTRAN) radiative transfer model, which simulates the interaction of thermal radiation with atmospheric gases, aerosols, and water vapor [39]. Key atmospheric parameters—including humidity, air temperature, geopotential height, and elevation—were derived from the National Aeronautics and Space Administration’s (NASA) Modern-Era Retrospective Analysis for Research and Applications, Version 2 (MERRA-2) reanalysis dataset [39]. These inputs enabled the model to estimate and compensate for atmospheric attenuation (e.g., absorption by water vapor and CO₂) and path radiance (upwelling and downwelling thermal emissions). The correction process ensured that the observed radiance values were accurately translated into surface-leaving radiance, a critical step for reliable land surface temperature (LST) derivation.

3.2.4 Computation of LST.

$$Emissivity_{Landsat} = c_{13} * Emmisivity_{ASTER13} + c_{14} * Emmisivity_{ASTER14} + c \quad (1)$$

Land Surface Temperature (LST) retrieval from Landsat thermal bands involves a series of radiative transfer corrections followed by temperature inversion [40]. According to [40], the process begins by isolating the surface-emitted radiance (L_s) from the top-of-atmosphere radiance (L) using atmospheric parameters (transmissivity τ , upwelling L_{\uparrow} , and downwelling L_{\downarrow} radiance) and spectral emissivity (ϵ) in Equation 2.

$$L_s = \frac{L - L_{\uparrow}}{\tau} - (1 - \epsilon)L_{\downarrow} \quad (2)$$

This corrected radiance was converted to LST by inverting the Planck function, which describes the relationship between radiance and temperature for a blackbody [41]. However, because Landsat’s thermal bands cover a broad wavelength range (10.4–12.5 μm for band 6) rather than a single wavelength, direct inversion of the Planck function introduces errors. To address this, a lookup table (LUT) approach was employed, where precomputed radiance values are generated across a temperature range (150–380 K) at fine intervals (0.01 K) using the sensor’s exact spectral response function. The observed radiance was matched to the closest value in the LUT through interpolation, yielding an accurate LST estimate. This method ensures robust temperature retrieval by accounting for both atmospheric influences and the sensor’s spectral characteristics.

3.2.5 Validation of the LST. Validation of Landsat-derived LST products was done using two independent datasets: [2] ground observations from four Surface Radiation Budget Network (SURFRAD) stations, and [3] thermal measurements from two inland water bodies (Salton Sea and Lake Tahoe) in the United States. or Landsat 5 [33]. Validation against SURFRAD sites showed a mean bias of 0.7 K with a root mean square error (RMSE) of 2.2 K, while Landsat 7 exhibited a slightly higher mean bias of 0.9 K (RMSE = 2.3 K). The validation against water bodies demonstrated even better agreement, with Landsat 5 showing a mean bias of -0.3 K (RMSE = 0.6 K) and Landsat 7 a mean bias of 0.4 K (RMSE = 0.7 K). These validation results confirm the reliability of the LST retrieval methodology, particularly for homogeneous surfaces like water bodies where the accuracy was within 1 K. The slightly higher errors observed at SURFRAD sites reflect the greater complexity of land surface emissivity variations in terrestrial environments.

3.2.6 Data access and processing in GEE. This study accessed pre-processed Landsat Level-2 Surface Temperature (LST) data from the Landsat 5 and Landsat 8 Collection 2 datasets available in Google Earth Engine (GEE). Data for the years 1995, 2007, 2015, and 2022 were retrieved from the Level-2 Surface Reflectance collection, which

includes atmospherically corrected surface temperature products. These products were derived from thermal infrared bands (Band 6 for Landsat 4–7 and Band 10 for Landsat 8–9) and were processed by the National Aeronautics and Space Administration (NASA) using the methodology described in previous sections, which includes atmospheric correction, emissivity adjustment, and LST retrieval [42]. To convert the digital numbers (DN) from the Landsat Collection 2 Level-2 Surface Temperature (ST) products into temperature values in degrees Celsius, the scaling factor provided in Equation 3 was applied within GEE.

$$ST (^{\circ}C) = ((DN \times 0.00341802) + 149.0) - 273.15 \quad (3)$$

Where $ST(^{\circ}C)$ is the Surface Temperature in Degrees Celsius, DN (Digital Number) are raw pixel values from Landsat thermal bands (ST_6 for Landsat 5, ST_10 for Landsat 8).

3.2.7 Correlation between LST and spectral indices. To extract Land Surface Temperatures (LSTs), the study processed thermal infrared data from Landsat imagery, converting digital numbers to top-of-atmosphere radiance and then to brightness temperature. These values were subsequently atmospherically corrected using a single-channel algorithm to derive the final LST measurements for the study area. The detailed extraction methodology is shown in the supporting material.

3.3 Surveys

This study employed surveys that utilised questionnaires administered to 150 street traders to understand their experiences of how (LST) affect their work and well-being. The corresponding author conducted all 150 interviews using Google Forms, targeting adults encountered in trading spaces from 16 August 2024 to 2 September 2024. The study targeted street vendors within spatially stratified transect sampling zones, encompassing central business districts (CBDs), low- and high-density residential areas, and industrial zones, to align empirical field observations with remotely sensed data. The survey targeted street traders who had been in business for over five years [43], aiming to gather their perspectives on temperature changes, workplace thermal conditions, trading experience (in terms of years and hours worked), and any health symptoms associated with rising temperatures. The prevalence of such symptoms across different land-use typologies was also a key focus. The questionnaires were translated into the local Ndebele language to enhance comprehension and participation, thereby improving data accuracy and reliability.

Surveys provide detailed information on street traders' perceptions, experiences, and behaviors. They provide offer insights into how land surface conditions, temperatures, and land-use patterns impact these traders. Additionally, surveys can be used to validate and calibrate remote sensing data, ensuring its accuracy and reliability [44].

4. Results and discussion

4.1 Spatial profiles of LST

Line Transects were utilised along varying land uses to show the different spatial profiles, as shown in Fig 3.

4.1.1 Spatial profile of LST in the CBD. Longitudinal analysis of CBD, LST revealed significant temporal variations (Fig 4). Winter LST measurements showed notable interannual fluctuations, recording 18.5°C in 1995, peaking at 26.9°C in 2007, then moderating to 22.4°C and 22.6°C in 2015 and 2022 respectively. Summer LST exhibited a clearer warming trajectory, increasing from 37.1°C in 1995 to 41.5°C in 2022, with intermediate values of 35.2°C in 2007 and 40.0°C in 2015. Spatial analysis identified consistent thermal depressions (3.2–4.1°C below CBD mean) in well-maintained green spaces like the Tower Block and City Hall areas, contrasting with thermal peaks in impervious surfaces with minimal vegetation cover [45].

The rising winter and summer temperatures highlight the effects of urbanisation and reduced vegetation cover, which can exacerbate heat stress in urban populations.

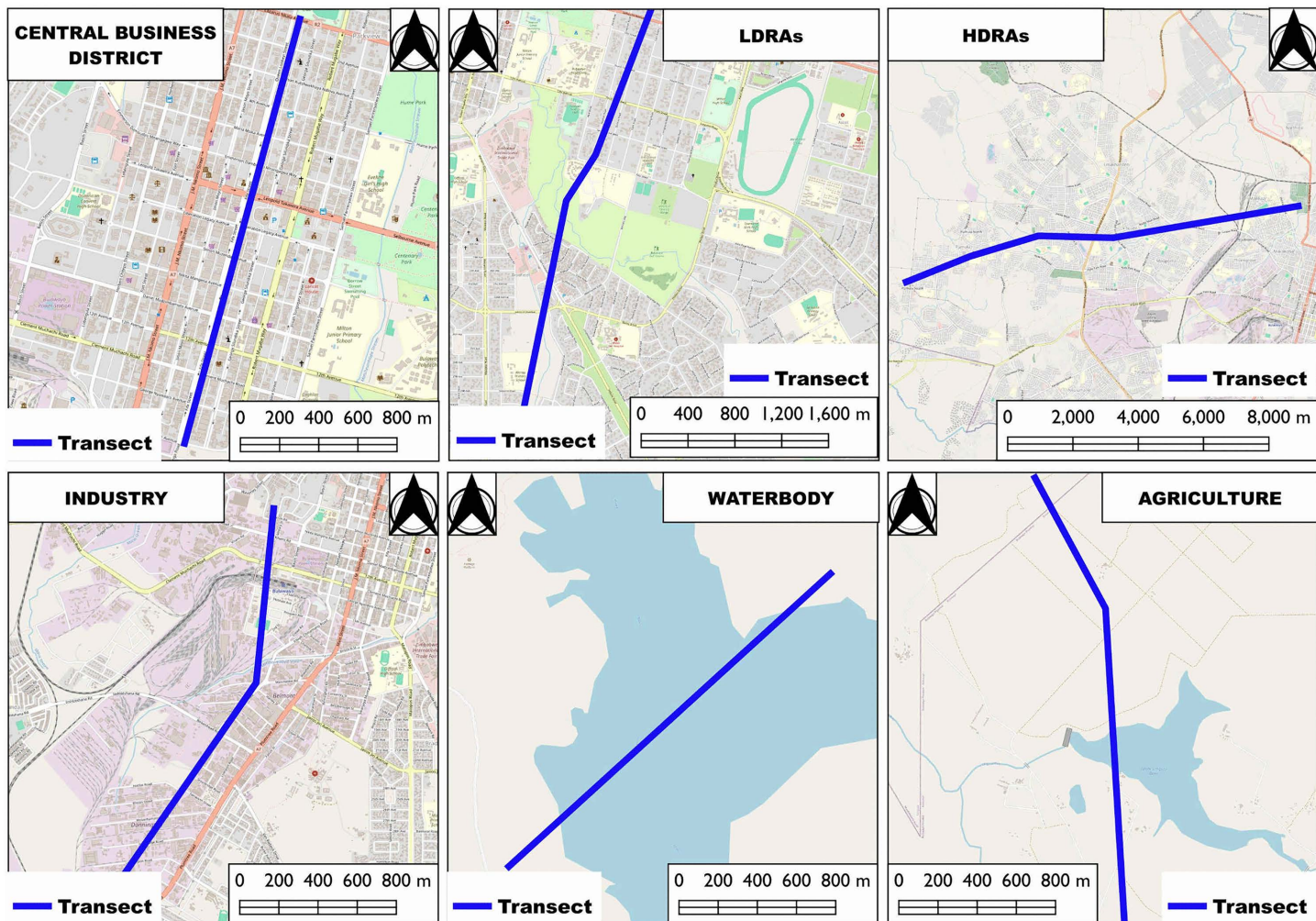


Fig 3. The location of transects that were employed to assess LST from various land uses in the city of Bulawayo.

<https://doi.org/10.1371/journal.pclm.0000716.g003>

4.1.2 Spatial profiles of LST in the low-density residential areas (LDRAs). Analysis reveals significant temporal and spatial variations in LST across Bulawayo’s urban landscape (Fig 5). Seasonal LST measurements demonstrate a clear warming trend in winter months, increasing from 19.2°C in 1995 to 21.1°C in 2022. Summer temperatures exhibited greater interannual variability, ranging from 34.2°C in 2007 to 38.8°C in 2022, with maximum temperatures consistently observed in non-vegetated areas of recreational spaces (golf courses: 42°C; sports grounds: 44°C). Spatiotemporal analysis of low-density residential areas (LDRAs) revealed distinct microclimatic regulation, characterised by significant vegetation cover- predominantly *Jacaranda mimosifolia* and other exotic species with high evapotranspiration rates; larger property sizes enabling private green space maintenance; active irrigation systems from boreholes and professionally maintained landscapes as the majority of households employing gardening staff.

These findings align with global research demonstrating that UHIs intensify in non-vegetated areas while green spaces provide cooling benefits [46].

4.1.3 Spatial profiles of LST in high-density residential areas (HDRAs). In winter, the mean LST measured 21.0°C, 28.1°C, 23.6°C, and 23.6°C for 1995, 2007, 2015, and 2022, respectively, while summer LST exhibited higher

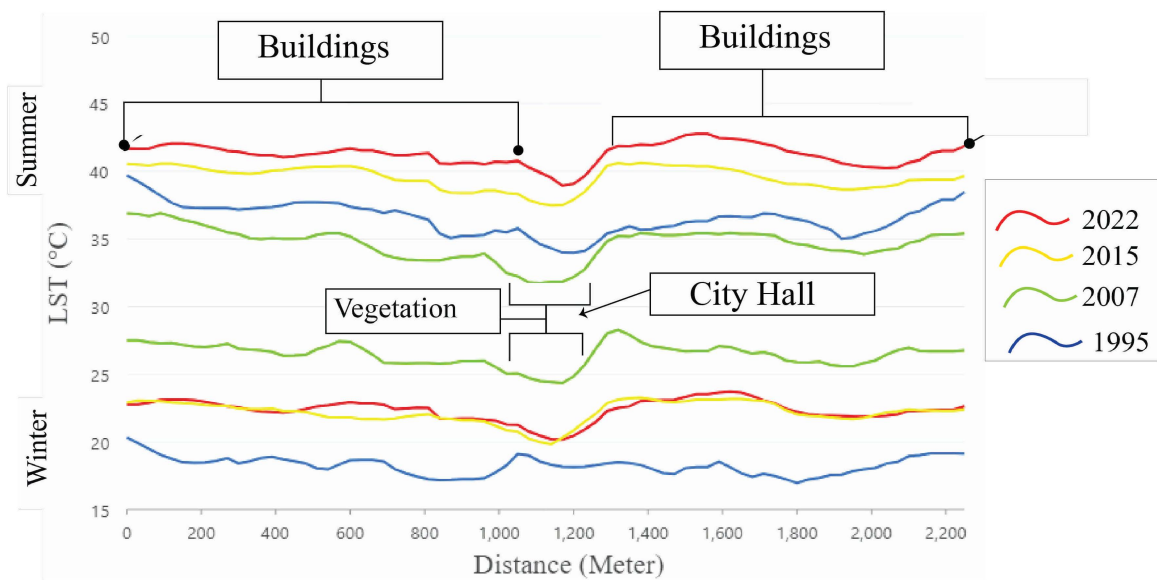


Fig 4. Spatial profiles of LST along the CBD of the City of Bulawayo.

<https://doi.org/10.1371/journal.pclm.0000716.g004>

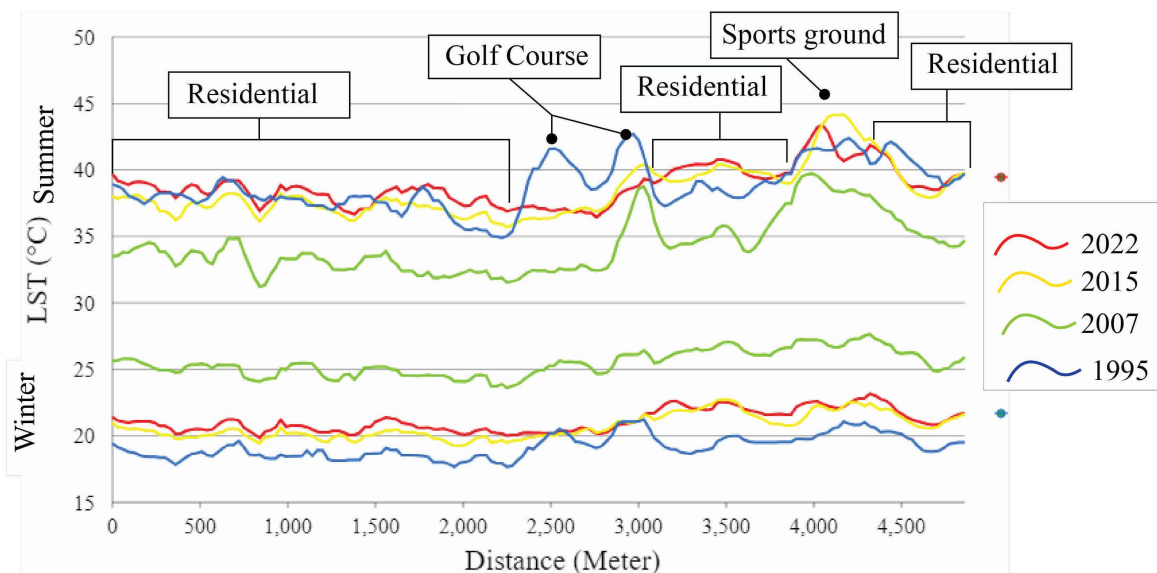


Fig 5. Spatial profile of LST along Low density areas in the city of Bulawayo.

<https://doi.org/10.1371/journal.pclm.0000716.g005>

thermal extremes at 39.5°C, 37.1°C, 41.8°C, and 43.4°C for the same years (Fig 6). These results demonstrate significant interannual and seasonal variability ($p < 0.05$), with summer temperatures showing an upward trajectory, particularly in high-density zones. Notably, LST in low-density areas remained below 40°C on average, whereas high-density residential areas consistently exceeded 42°C (Fig 9), a pattern strongly linked to vegetation disparities—low-density regions retained higher green cover, while high-density areas exhibited minimal vegetation. Spatial profiles further revealed moderate

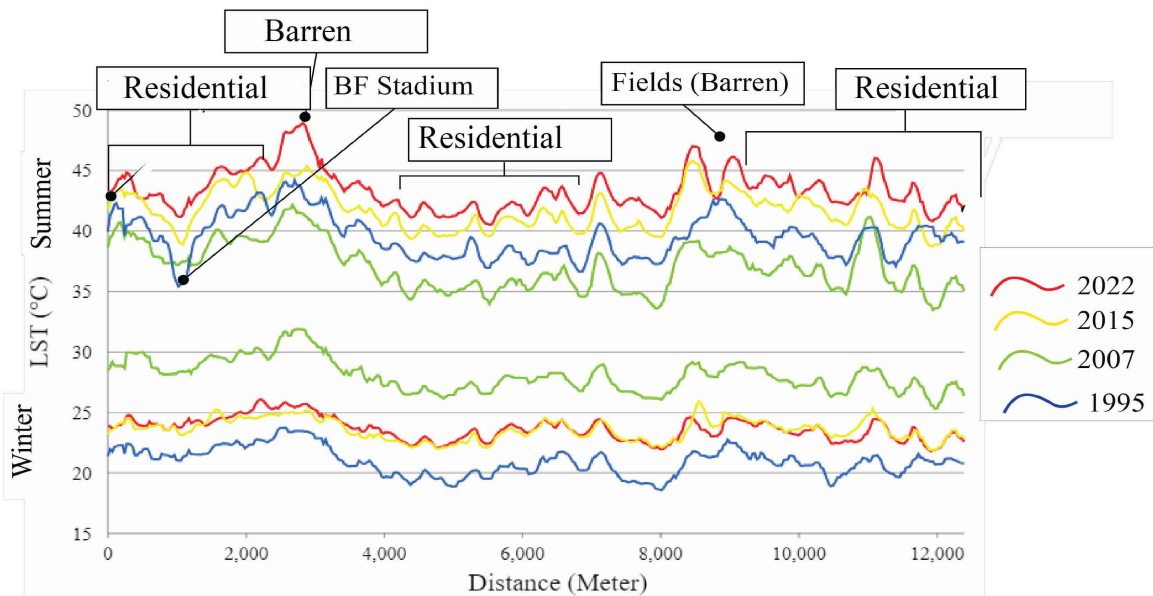


Fig 6. Spatial profiles of LST along high-density areas in the City of Bulawayo.

<https://doi.org/10.1371/journal.pclm.0000716.g006>

thermal peaks in high-density zones, where open spaces, such as sports grounds with bare soil and artificial turf, amplified local warming due to reduced evapotranspiration and increased heat retention.

The observed patterns for Bulawayo align with global urban climate dynamics worldwide revealing 2–4°C differences between low- and high-density zones. The extreme LST (>42°C) in recreational spaces corroborate findings from the globe where artificial turf reached 60°C surface temperatures, underscoring the global ubiquity of surface material-driven heating. These parallels underscore the transcontinental validity of UHI drivers, from vegetation deficits to anthropogenic land cover [47,48].

4.1.4 Spatial profiles of LST along water bodies. The mean winter LST for water bodies varied across the years, recording 16.5°C (1995), 20.4°C (2007), 17.9°C (2015), and 18.2°C (2022). In contrast, summer LSTs were significantly higher, reaching 29.2°C (1995), 25.5°C (2007), 30.0°C (2015), and 31.9°C (2022). Peaks and depressions were noted in the water bodies due to the variations that exist naturally. Lower LSTs were recorded at the centre and deep ends of the water bodies and these increased as one approached the banks. Most of the waterbodies in Bulawayo have been affected by the invasive water hyacinth especially at the banks. These alter LST significantly as they become warmer than at the centre.

4.1.5 Spatial profile of LST in the agricultural areas. Agricultural areas in Bulawayo exhibited notable LST variations, with winter means peaking at 27.5°C (2007) before stabilising around 23.6°C (2022), while summer temperatures showed consistent warming from 36.1°C (1995) to 42.8°C (2022), reflecting regional climate warming trends [29,36]. The thermal patterns demonstrated clear land-use influences, with actively cropped fields exhibiting 3–5°C lower LST than fallow plots due to vegetation-mediated cooling through evapotranspiration [49]. Notably, irrigated agricultural zones near water bodies (e.g., Umguza Dam) maintained significantly lower temperatures (~4–6°C) than non-irrigated areas (Fig 7), highlighting the combined cooling effects of soil moisture and vegetation cover [49].

These findings align with recent studies on agro-thermal dynamics in semi-arid regions, emphasising the climate adaptation potential of sustainable land management practices in urban peripheries.

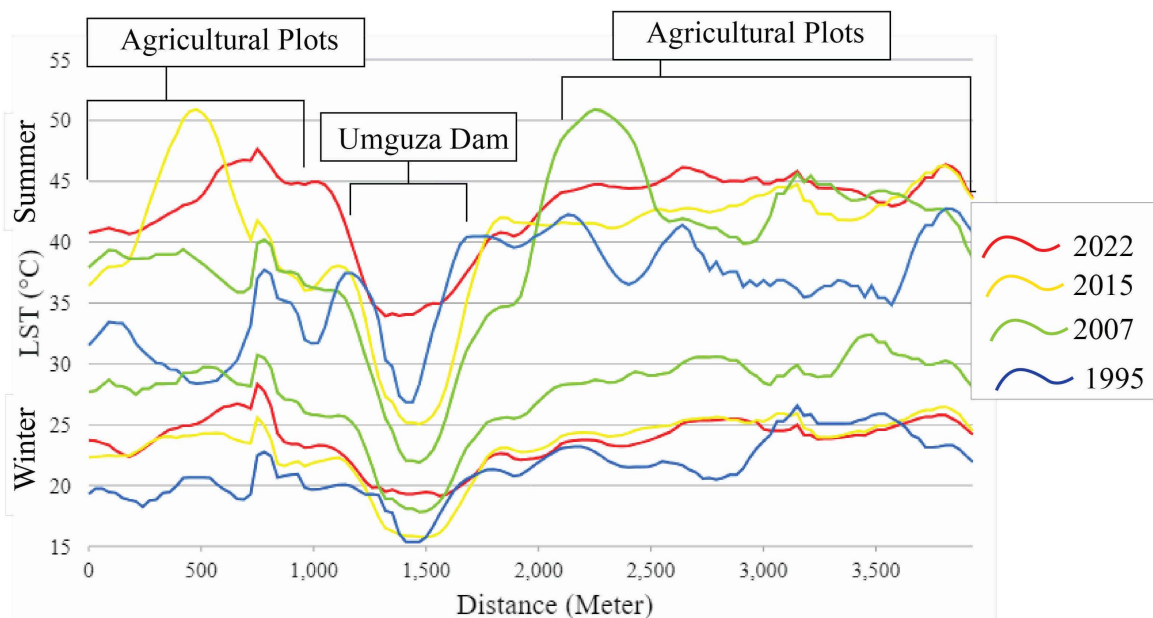


Fig 7. Spatial profiles of LST in the Agricultural areas in the city of Bulawayo.

<https://doi.org/10.1371/journal.pclm.0000716.g007>

4.1.6 Spatial profile of LST in the industrial areas. Winter averages were 20.9°C (1995), 28.2°C (2007), 23.8°C (2015), and 24.0°C (2022). Summer temperatures remained consistently high, with values of 39.3°C (1995), 37.2°C (2007), 41.9°C (2015), and 43.4°C (2022) as shown in Fig 8.

These indicate variations over years and different seasons with LST being generally higher than those of the CBD and LDRAs. LST dropped where vegetation cover improved. The observed inverse relationship between LST and industrial areas aligns with established UHI mechanisms [50] and was corroborated by street traders' reports of higher thermal discomfort in industrial zones. These findings underscore the need for targeted heat mitigation strategies in industrial areas, particularly through green infrastructure implementation.

4.2 Land surface temperature status

The analysis of Land Surface Temperature (LST) trends in Bulawayo from 1995 to 2022 reveals significant seasonal variations, marked by pronounced warming in both winter and summer. During winter, the mean LST increased from 20.9°C in 1995 to 23.4°C in 2015 and 2022. This trend was characterised by an extreme peak of 27.5°C in 2007, suggesting intermittent but intensifying warming episodes (Fig 9). The anomalously warm temperatures in 2007 can be as a result of the La Niña and EL Nino effect that occurred from 2006 to 2008 [51]. In contrast, summer LST exhibited a more consistent upward trajectory, rising from 40.5°C in 1995 to 43.5°C in 2022, with record-breaking maxima in 2007 (53.1°C) and 2015 (57.7°C). The year 2007 was an El Niño year, and the stronger event in 2015 triggered a severe drought and reduced cloud cover. This amplified solar heating and desiccated soils, thereby raising LST [51–53]. The stability of the winter LST standard deviation (~1.1–1.6) implies uniform warming across the region, whereas the slight increase in summer LST variability (Std: 2.0–2.6) points to greater thermal instability. This instability is likely driven by heterogeneous urban surface properties and suggests intensified urban heat island (UHI) effects. The persistent LST increases align with Bulawayo's urban expansion, where impervious surfaces (e.g., asphalt, concrete) with low albedo and high thermal capacity replace natural vegetation [54].

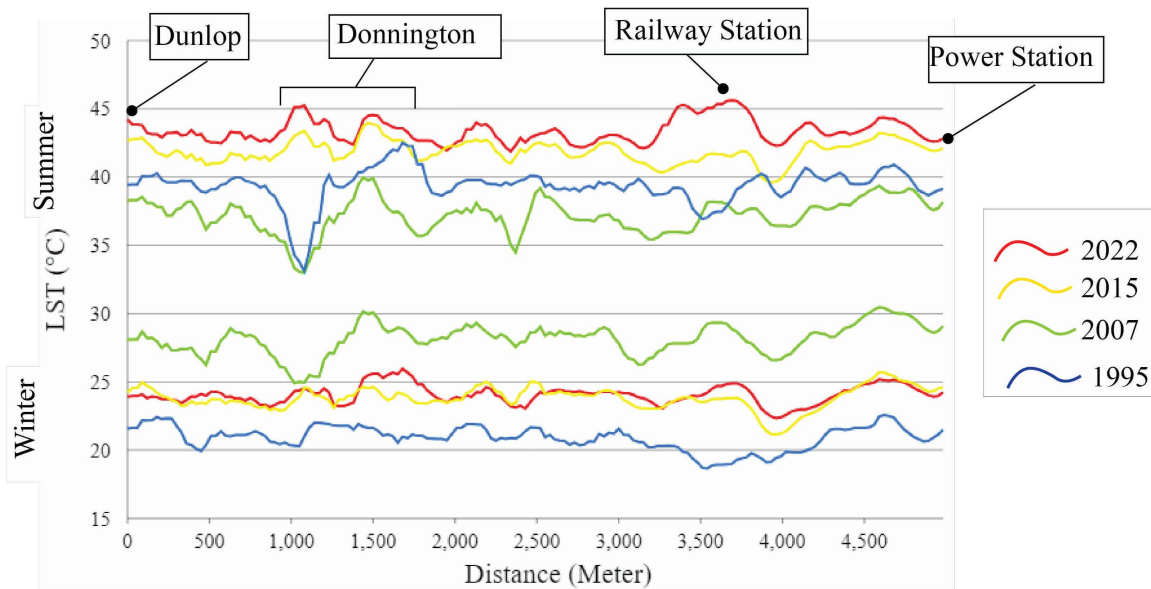


Fig 8. Spatial profiles in the Industrial areas of the city of Bulwayo.

<https://doi.org/10.1371/journal.pclm.0000716.g008>

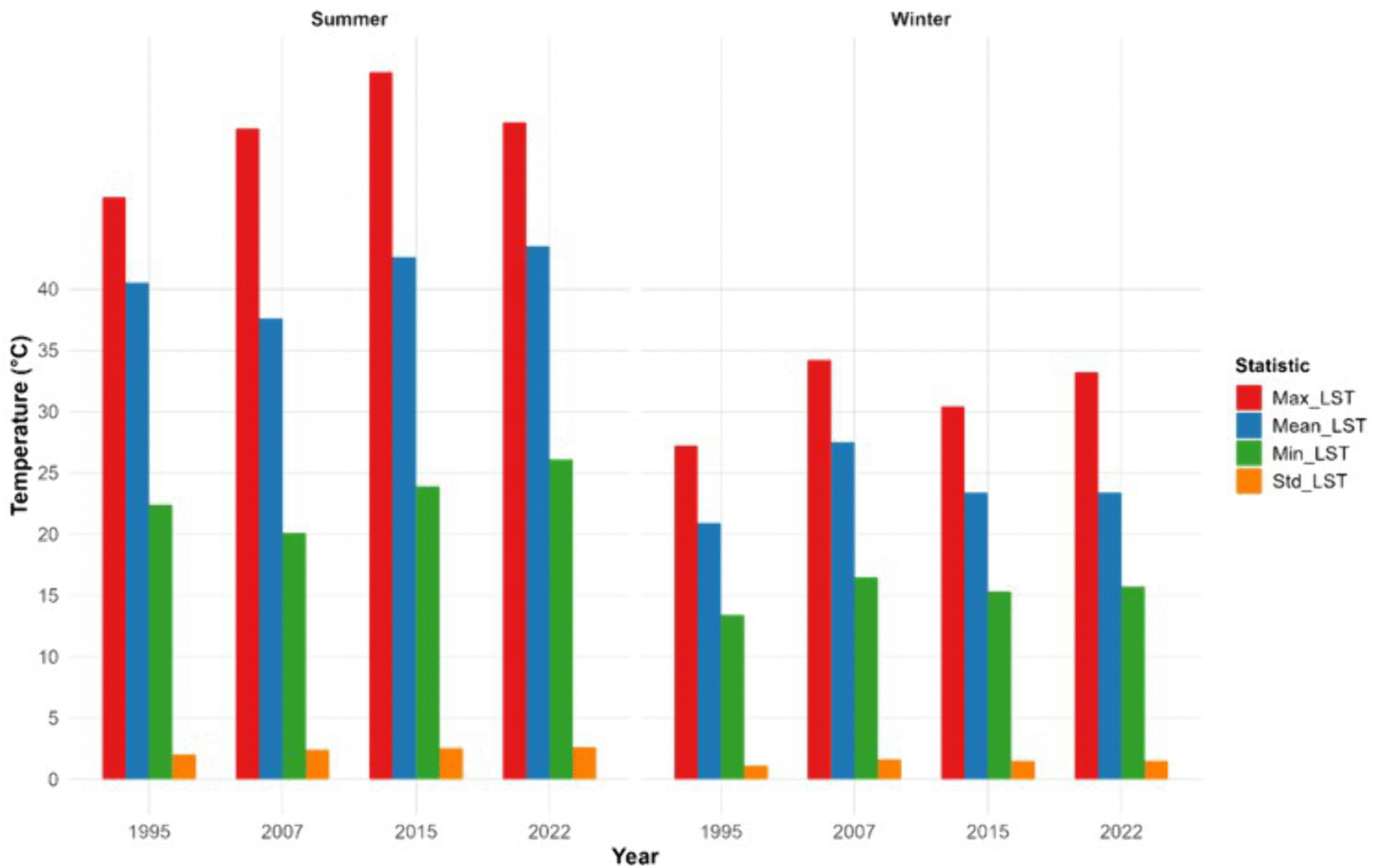


Fig 9. The status of Minimum, Maximum and standard deviation for LST for 1995, 2007, 2015 and 2022.

<https://doi.org/10.1371/journal.pclm.0000716.g009>

The extreme summer spikes (e.g., 2007, 2015) may reflect the compounded effects of global climate change and localised land-cover changes [55]. These findings are consistent with global observations of urbanisation-driven warming [45,56].

Rising land surface temperatures significantly impair street traders' livelihoods by reducing their working hours and increasing heat-related health risks. These findings underscore the urgency for urban policymakers to implement adaptive measures—such as designated shaded vending zones and public cooling stations—to safeguard this vulnerable workforce.

4.3 Spatial distribution of LST

The spatial distribution of land surface temperature (LST) in Bulawayo exhibits pronounced thermal heterogeneity, driven primarily by land cover and urbanisation. Winter LST were markedly colder in 1995 than in 2007, 2015, and 2022. However, 2007 showed anomalous cooling attributable to localised climatic variability or specific land-use changes [29,36]. Persistent cold spots were identified in water bodies, agricultural areas, the Central Business District (CBD), and low-density suburbs, where evapotranspiration and vegetative cover moderate temperatures [50]. Spatial profile analysis revealed a strong inverse correlation between LST and tree canopy density; low-density urban zones exhibited significantly lower LST than high-density or industrial areas. This pattern aligns with established mechanisms of evapotranspiration and shade-driven microclimatic regulation, corroborating findings from prior studies on urban heat mitigation [57]. Conversely, hotspots dominate high-density residential and industrial zones, where impervious surfaces (e.g., asphalt) reduce albedo and amplify heat retention [55].

The increase in hotspot area and the concomitant decline in cold spots from 1995 to 2022 (Fig 10 and Fig 11) confirm escalating surface urban heat island (SUHI) effects, a trend consistent with global UHI dynamics. Street traders' reports corroborate these findings, identifying high-density and industrial areas as perceptibly hotter than the tree-shaded CBD and low-density zones. The Joshua Mqabuko Nkomo Airport emerged as the most extreme hotspot in the study area, a phenomenon attributable to its extensive heat-absorbing tarmac. These results underscore the urgency of implementing targeted urban greening and cool roofing interventions in high-heat zones to mitigate thermal disparities.

4.4 Relationship between LST and NDVI, mNDWI, DBI and DBSI

This study rigorously investigates the spatiotemporal relationships between land surface temperature (LST) and key environmental indices—Normalized Difference Vegetation Index (NDVI), modified Normalized Difference Water Index (mNDWI), Dry Built-up Index (DBI), and Dry Bare Soil Index (DBSI)—to unravel the complex interplay of urbanization, hydrology, and vegetation dynamics on thermal landscapes see Fig 12.

4.4.1 Relationship between LST and NDVI. The analysis of 1,000 sample points revealed a significant negative correlation between LST and NDVI in both winter ($r = -0.53$, $r^2 = 0.28$, $p < 0.0001$) and summer ($r = -0.35$, $r^2 = 0.13$, $p < 0.0001$), reinforcing vegetation's critical role in urban temperature regulation. The stronger correlation in winter suggests an enhanced cooling efficiency during drier periods, due to reduced competition for soil moisture and greater transpirational cooling effects. These findings corroborate global evidence that green spaces (e.g., parks and vegetated areas) consistently exhibit lower LST than built-up environments [50], with canopy cover being particularly effective in mitigating surface urban heat islands (SUHIs) [46,58,59]. The results underscore the importance of preserving and expanding green infrastructure as a key climate adaptation strategy, especially during water-limited seasons [59].

Relationship between LST and DBSI

The analysis revealed strong positive correlations between LST and the Dry Bare-Soil Index (DBSI) in Bulawayo for both winter ($r = 0.69$, $r^2 = 0.47$, $p < 0.0001$) and summer ($r = 0.62$, $r^2 = 0.39$, $p < 0.0001$), demonstrating that bare, dry surfaces significantly elevate urban temperatures. These findings align with similar observations in Raipur City, India ($r = 0.35$),

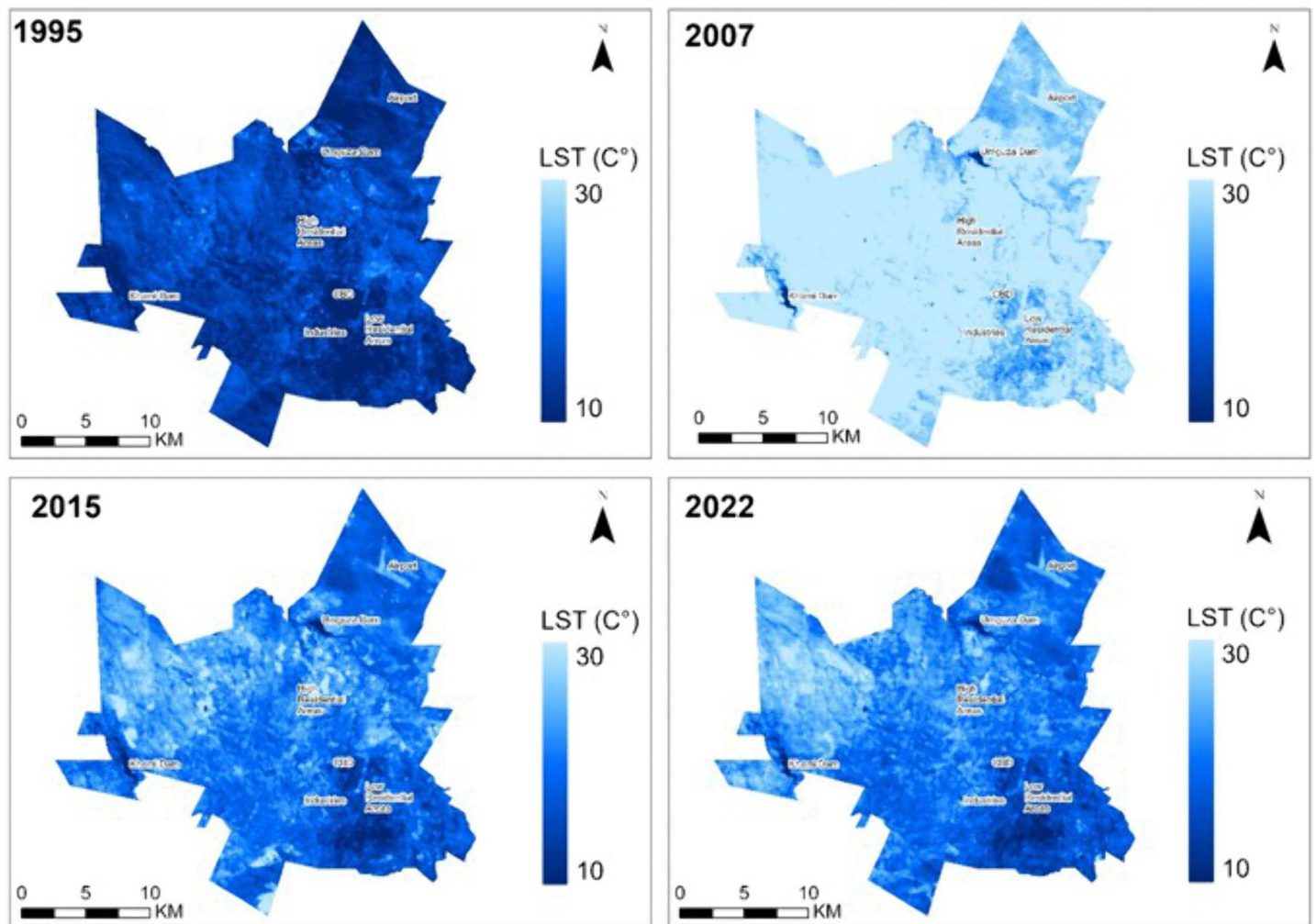


Fig 10. Spatial distribution of Winter LST for the years 1995, 2007, 2015, 2022.

<https://doi.org/10.1371/journal.pclm.0000716.g010>

though the correlations in Bulawayo are more pronounced. This discrepancy may be attributable to differences in urban morphology or climatic conditions [50]. The strength of these correlations confirms that such surfaces are a major contributor to urban heating, creating dangerous microclimates for street traders. This risk is particularly acute in high-DBSI zones like high-density residential areas (HDRAs), where shade is limited. The consistency of this relationship across seasons suggests that street traders face year-round thermal stress, a phenomenon primarily driven by the prevalence of bare surfaces and impervious landscapes. Consequently, the DBSI-LST relationship provides a precise and valuable planning tool for mitigating trader health risks through targeted surface material interventions.

4.4.2 Relationship between LST and mNDWI. The analysis revealed significant negative correlations between the modified Normalised Difference Water Index (mNDWI) and land surface temperature (LST) in Bulawayo. These correlations were stronger in summer ($r=-0.33$, $r^2=0.11$, $p<0.0001$) than in winter ($r=-0.25$, $r^2=0.06$, $p<0.0001$). The stronger summer association confirms that water-rich areas (e.g., rivers, reservoirs, and wetlands) provide more effective urban heat mitigation during periods of peak temperature [60]. For street traders, proximity to such water bodies or to designed blue-green infrastructure (e.g., shaded canals, misting stations) could reduce heat exposure, which has been linked to productivity losses

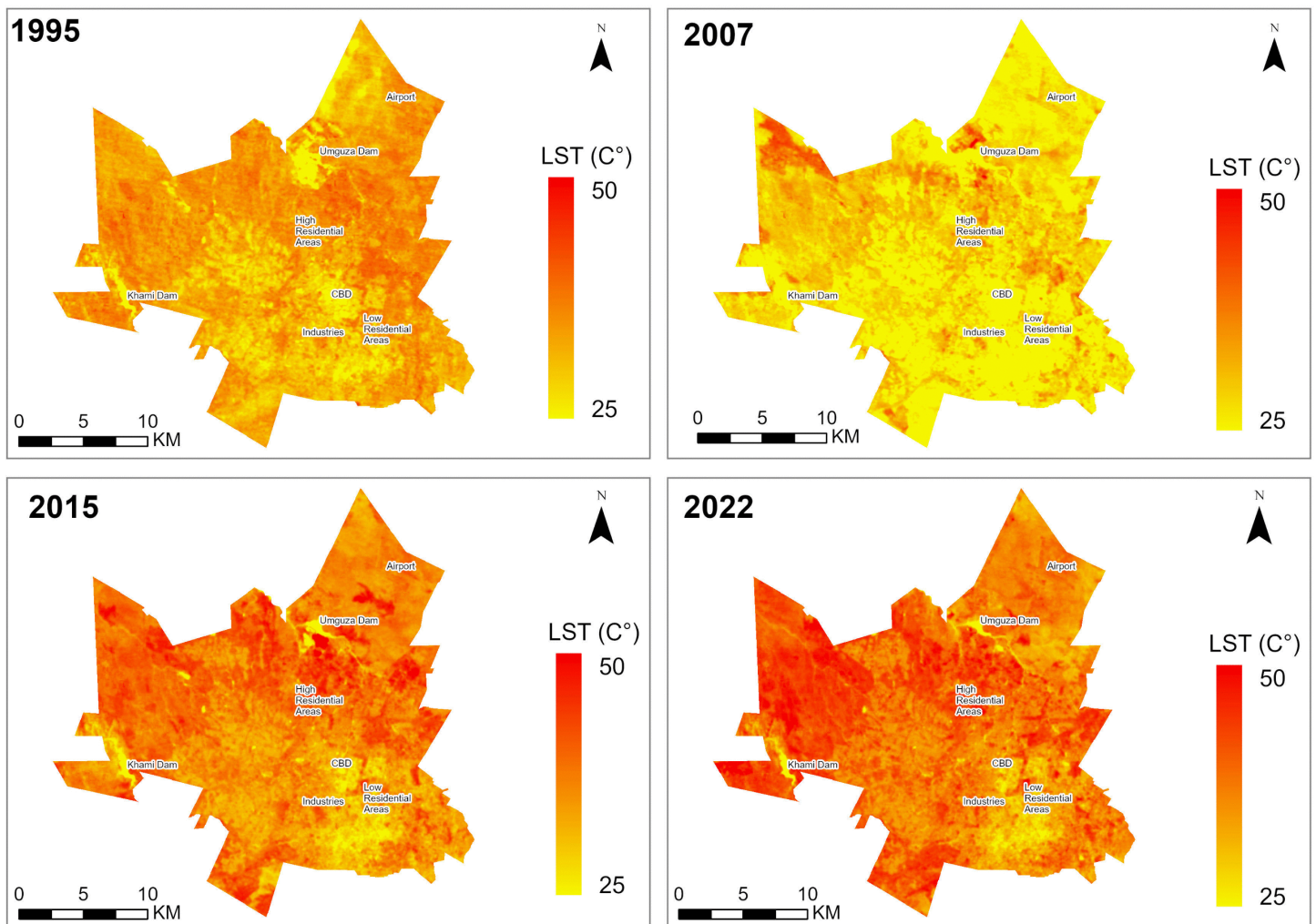


Fig 11. Spatial distribution of summer LST for the years 1995, 2001, 2015 and 2022.

<https://doi.org/10.1371/journal.pclm.0000716.g011>

of 15–30% at temperatures exceeding 35°C [60]. The weaker, yet still significant, winter correlation suggests a persistent but diminished cooling effect from water throughout the year. Consequently, street traders in water-scarce zones face compounded heat stress in summer due to a lack of these natural buffers. The consistent mNDWI–LST relationship underscores the need for urban planning strategies that co-locate trading hubs near existing water features or retrofit cooling oases in water-poor areas.

4.4.3 Relationship between LST and DBI. The analysis demonstrated consistent positive correlations between the Dry Built-up Index (DBI) and land surface temperature (LST) across seasons (winter: $r=0.45$, $r^2=0.20$; summer: $r=0.47$, $r^2=0.22$; $p<0.0001$). These robust relationships confirm that impervious surfaces elevate local temperatures year-round, with built-up areas explaining 20–22% of LST variability. This finding provides critical insights for managing thermal environments in cities and for protecting vulnerable outdoor workers. While built-up coverage explains approximately 20% of LST variation—a finding that aligns with those of [61,62]—the moderate r^2 values highlight the importance of complementary factors such as building materials, urban geometry, and anthropogenic heat in driving microclimates. These results emphasise the need for integrated heat mitigation strategies in urban planning, particularly through improved building design and material selection.

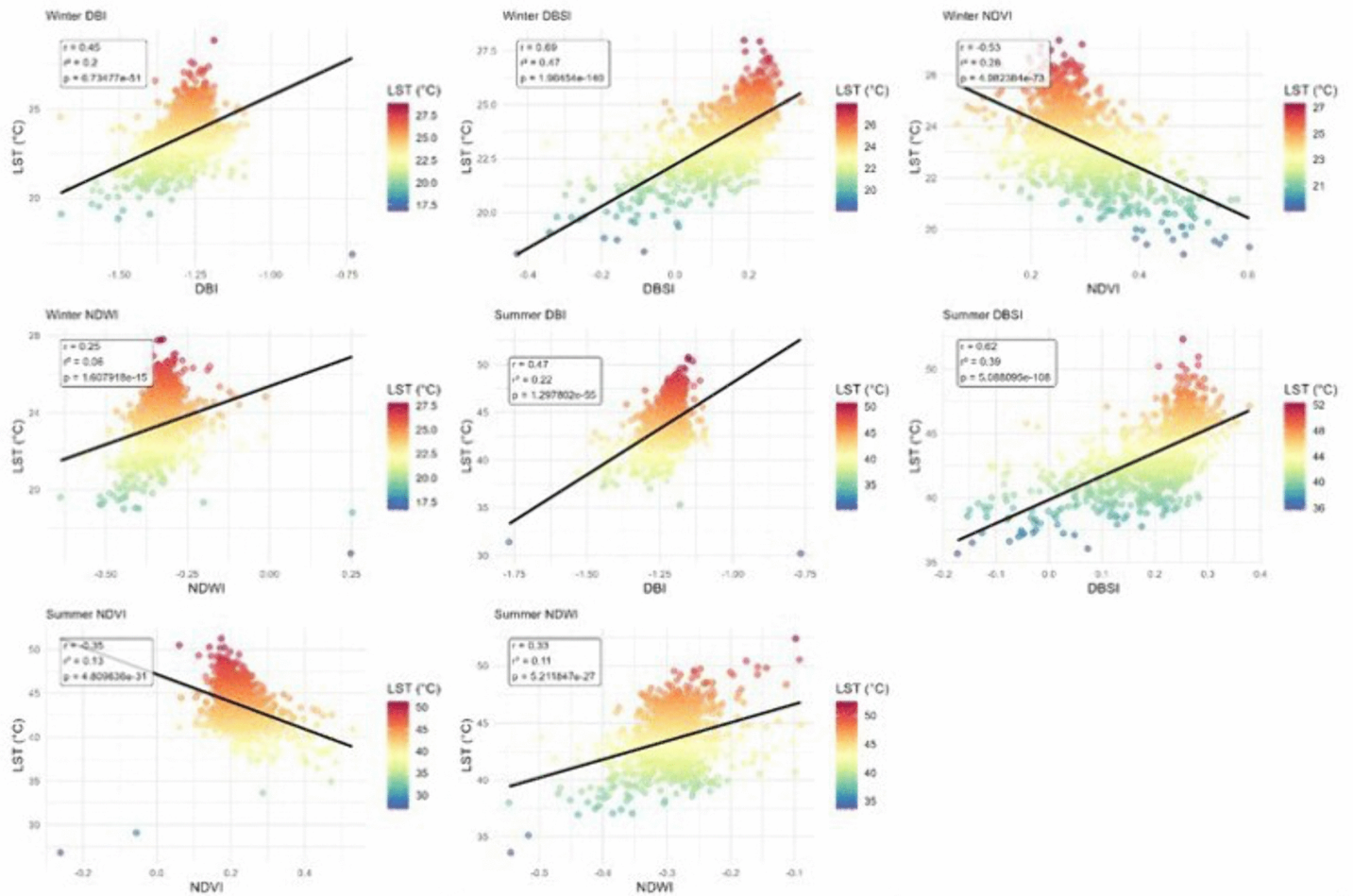


Fig 12. Relationship between Winter LST and NDVI, mNDWI, DBSI and DBI.

<https://doi.org/10.1371/journal.pclm.0000716.g012>

4.4.4 Built-up vs non-built-up changes. Quantitative geospatial analysis reveals a marked exponential increase (+228%) in built-up areas across Bulawayo, Zimbabwe, between 1984 and 2022, concurrent with a 29.28% decline in non-built-up land cover (e.g., agricultural land, vegetation, and bare surfaces), as demonstrated by multitemporal satellite-derived classifications in Fig 13. These findings align with recent work by [20], underscoring the rapid transformation of peri-urban landscapes into impervious surfaces at a rate exceeding regional urbanisation trends. The primary drivers of this shift, identified through integrated spatial-statistical modelling, are: (1) accelerated urbanisation linked to population growth (2.7% annual increase; ZimStat 2022); (2) climate-induced pressures on agrarian livelihoods, driving rural-urban migration; (3) evolving land-use policies favouring densification; and (4) expanding informal settlements due to housing deficits.

This unprecedented land cover transition raises critical concerns about ecosystem service loss, urban heat island (UHI) intensification, and groundwater recharge deficits. The study advocates for the urgent integration of satellite-based monitoring into adaptive land-use planning frameworks to balance developmental needs with ecological resilience—a key policy priority for rapidly urbanising cities in the Global South.

4.4.5 Long-term trends of LST from MODIS. The long-term analysis of land surface temperature (LST) trends in Bulawayo reveals heterogeneous warming patterns (see Fig 14 and Fig 15), with significant increases concentrated in December and the



Fig 13. Showing the landcover changes of Bulawayo for 1995, 2007, 2015 and 2022.

<https://doi.org/10.1371/journal.pclm.0000716.g013>

October–December (OND) season, while most other periods show non-significant trends. Specifically, December mean and minimum LST, along with the OND minimum LST, show statistically significant increases ($p < 0.05$). This suggests intensifying heat stress during Bulawayo’s summer months, a phenomenon likely exacerbated by urban heat island effects in high-density and commercial zones where street traders operate. Rising minimum temperatures (e.g., Sen’s Slope = 0.326 for December Min LST) indicate warmer nights, which may disrupt thermal recovery for traders and residents reliant on informal outdoor markets. The results reveal non-significant trends in other seasons, for example, March and September exhibit seasonal stability. Concurrently, the annual mean LST shows a slight, non-significant rise. This pattern underscores that warming is concentrated in specific periods, aligning with peak dry-season trading activities in December (see [Table 2](#)).

These findings align with regional climate observations in southern Africa, where late-year warming has been linked to shifts in rainfall patterns and increased atmospheric aridity. The observed spatial and temporal variability in warming suggests complex interactions between local urban factors and regional climate dynamics.

The statistically significant rise in December mean LST ($p = 0.014$) and minimum LST ($p = 0.004$) suggests intensified late-year heating. This pattern may be caused by multiple factors, including the delayed onset of summer rains—which

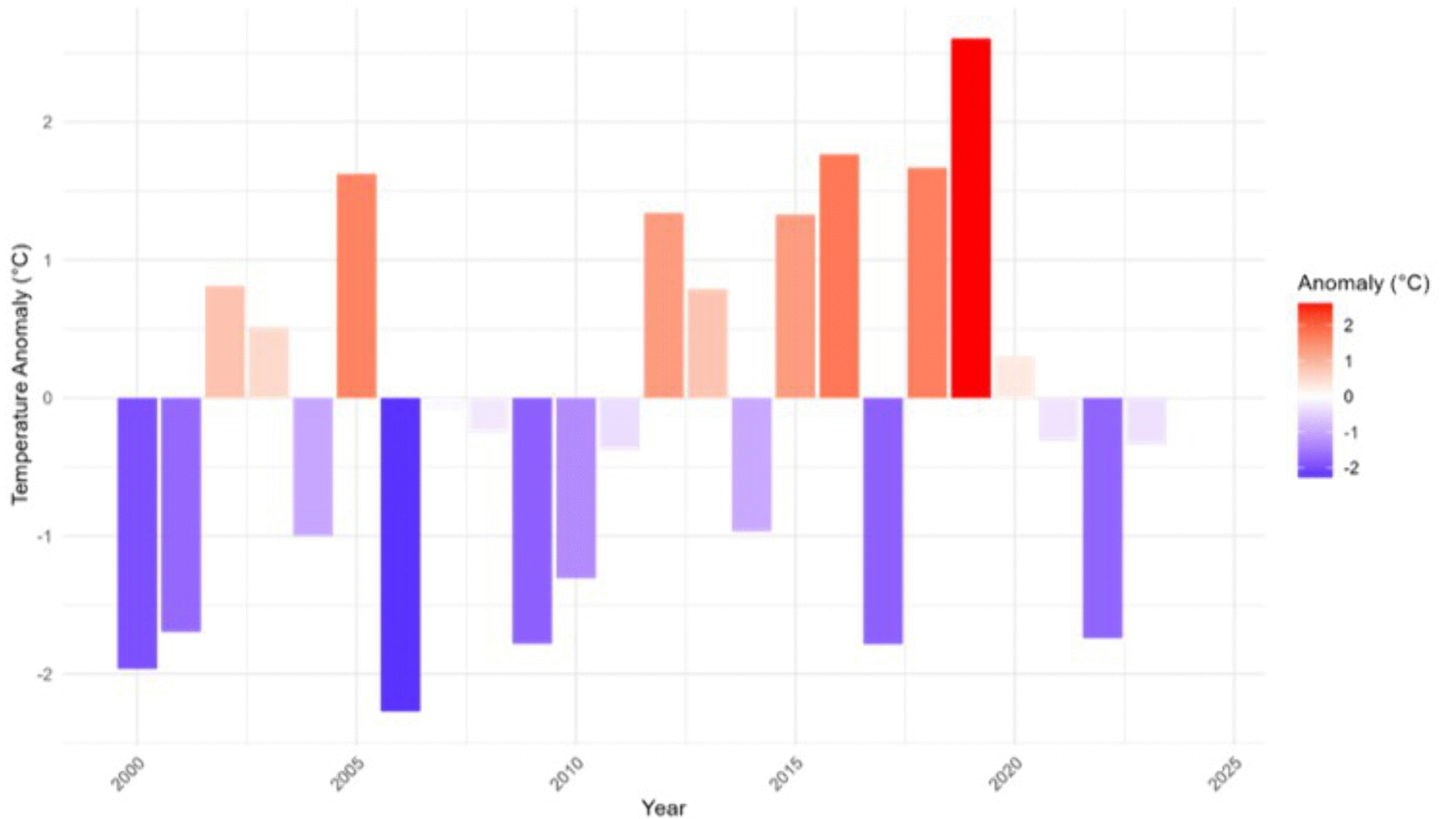


Fig 14. Yearly temperature anomalies for the City of Bulawayo.

<https://doi.org/10.1371/journal.pclm.0000716.g014>

reduces evaporative cooling [29,36]—and urban heat island (UHI) intensification, as built-up surfaces retain more heat during drier periods. Furthermore, the increase in the October–November–December (OND) see also (Fig 16) season’s minimum LST ($p=0.002$) likely reflects reduced night-time cooling, a phenomenon consistent with global observations of urban heat storage effects. These findings highlight Bulawayo’s vulnerability to late-year temperature extremes.

In contrast to the significant late-year warming, the lack of significant warming trends from March to August suggests stable thermal conditions during the cooler months. This stability may result from persistent cloud cover or land-atmosphere feedbacks that moderate temperature fluctuations [50]. The marginal annual LST increase ($p=0.272$) presents an interesting contrast to the stronger warming observed in other African cities, a difference potentially attributable to Bulawayo’s semi-arid climate providing a buffering effect against extreme temperature shifts. This differential warming pattern underscores the importance of accounting for local climatic contexts in urban heat studies.

The heterogeneous warming patterns in Bulawayo, with significant temperature increases concentrated in December and the OND season, highlight a critical and temporally precise climate risk that exacerbates urban heat stress [49]. Several key drivers may explain the observed temperature trends in Bulawayo. Land-use changes, particularly urban expansion, likely contribute to localised warming, especially in December when vegetation cover is minimal [49]. The statistically significant rise in minimum land surface temperature (LST) is particularly consequential, as it indicates warmer nights that disrupt the crucial physiological recovery period for heat-exposed populations, a phenomenon increasingly linked to adverse health outcomes in urban areas worldwide. This intensification of late-year

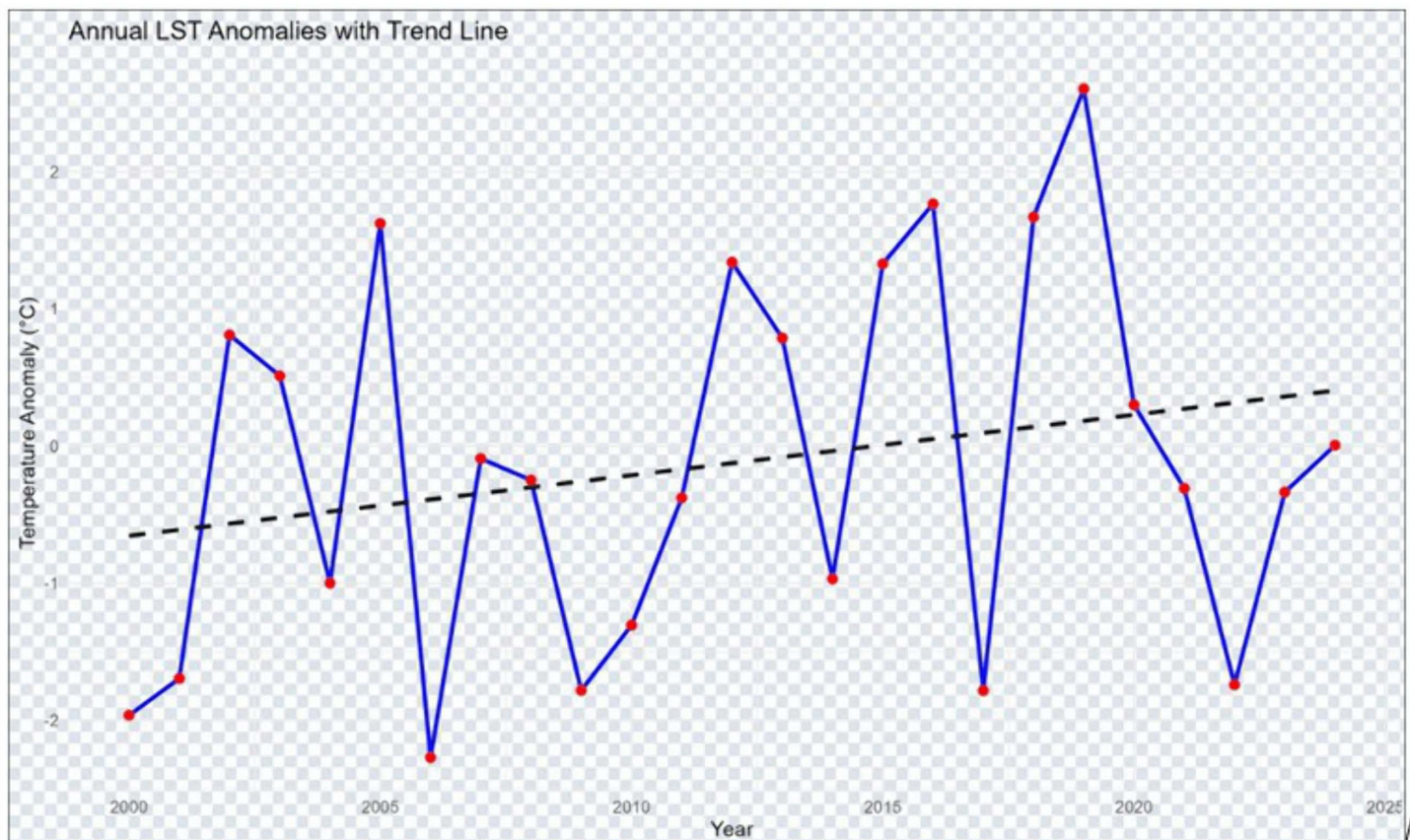


Fig 15. Yearly temperature anomalies for the City of Bulawayo.

<https://doi.org/10.1371/journal.pclm.0000716.g015>

Table 2. Long-Term LST Trends for Bulawayo (2000–2024).

Variable	Sen's Slope	Kendall's Tau	p-value	Trend Interpretation
December Mean LST	0.248	2.45	0.014*	Significant Increase
December Min LST	0.326	2.87	0.004**	Significant Increase
OND Min LST	0.366	3.15	0.002**	Significant Increase
March Mean LST	0.148	1.56	0.118	Non-Significant Increase
September Mean LST	-0.04	-0.72	0.469	Non-Significant Decrease
Annual Mean LST	0.053	1.1	0.272	Non-Significant Increase

<https://doi.org/10.1371/journal.pclm.0000716.t002>

heat aligns with broader observations of urban heat island (UHI) dynamics, where built-up areas with minimal vegetation exhibit amplified warming due to heat storage and reduced evaporative cooling, especially preceding seasonal rains [46,59]. The spatial correlation between MODIS-derived LST hotspots (3–5°C warmer), low NDVI, and clusters of self-reported morbidity symptoms provides robust evidence that urban landscape features directly mediate health risks. This pattern confirms that for cities in semi-arid regions like Bulawayo, warming is not uniform but is instead concentrated in key seasons, thereby exposing street traders and outdoor workers to disproportionate health hazards during peak economic activity periods, underscoring the urgent need for seasonally targeted adaptation strategies.

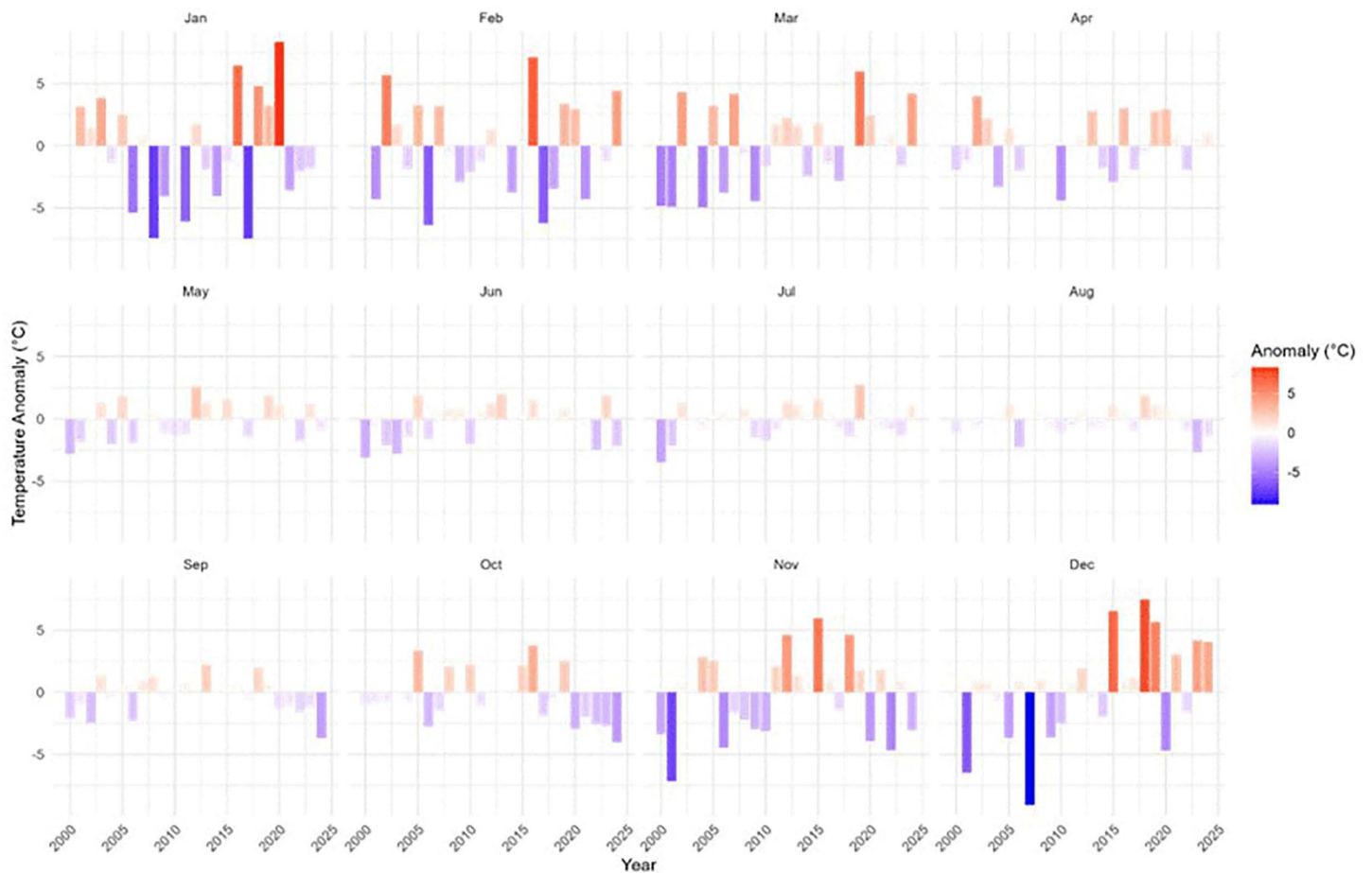


Fig 16. Monthly temperature anomalies for the city of Bulawayo.

<https://doi.org/10.1371/journal.pclm.0000716.g016>

4.5 Evidence from the survey

4.5.1 Perceived temperatures and symptoms. The health survey conducted among Bulawayo’s street traders reveals significant heat-related morbidity during the summer months (see Fig 17). Nearly all respondents (98.7%) reported experiencing headaches, followed by high rates of dehydration (84.7%), profuse sweating (84%), and fatigue (79.3%). The results indicate that traders operating in the central business district (CBD), industrial areas, and high-density residential areas experienced more heat-related symptoms than those in low-density areas. A majority of these traders reported experiencing at least five out of eight documented heat-related symptoms in their areas of operation. The raw data of the street traders responses is attached as [S1 Table](#).

Street vendors working in high Dry Built-up Index (DBI) zones (e.g., markets near paved roads in the CBD or near concrete buildings in industrial areas) face prolonged heat exposure, which increases the risk of dehydration, heat exhaustion, and cardiovascular strain.

The concentration of symptoms in high-density and built-up areas points directly to the urban heat island (UHI) effect as the primary driver. These zones, characterized by impervious surfaces (high DBI), trap and radiate heat, exposing vendors to extreme radiant—not just ambient—heat. This results in chronic physiological strain that impairs health and productivity, far exceeding the risk of acute heatstroke [13,23]. The high symptom burden—with most traders

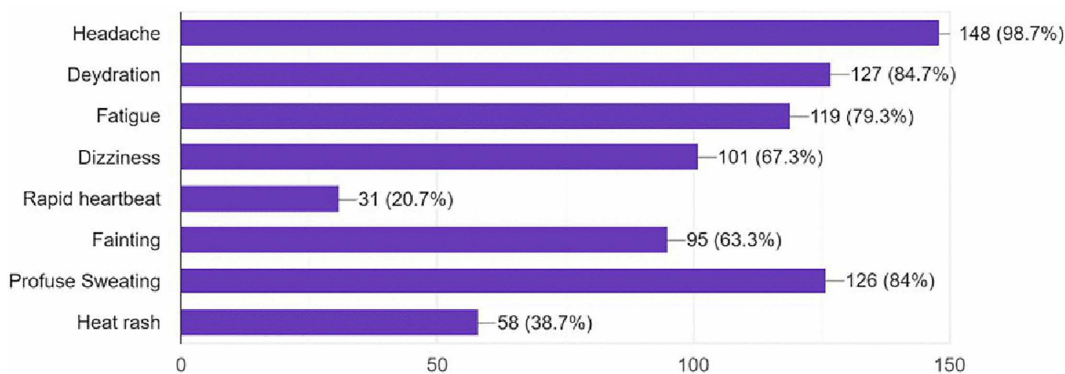


Fig 17. Showing how often the traders responded on each symptom.

<https://doi.org/10.1371/journal.pclm.0000716.g017>

experiencing at least five—shows heat illness is not a series of isolated symptoms but a cascade of co-occurring conditions. This reflects severe physiological strain and frames extreme heat as a critical occupational hazard and workers’ rights issue [23].

Perceptual data from street traders identified significantly cooler temperatures in vegetated, low-density areas. These reports validate the concurrent spatial and quantitative analyses, which demonstrate a consistent pattern of lower land surface temperatures in low-density residential zones compared to adjacent high-density and commercial areas. The study observed a stark contrast in the prevalence of heat-related morbidity: traders in high-density and central business district (CBD) areas reported experiencing symptoms habitually, whereas their counterparts in low-density areas reported only occasional occurrences.

The stark contrast in heat morbidity, with traders in vegetated low-density areas reporting only occasional symptoms compared to the habitual suffering in high-density zones, validates urban greenery as critical health infrastructure. This demonstrates that trees mitigate the urban heat island effect through shading and evapotranspiration [46,59], creating a measurably safer microclimate. Consequently, equitable access to green space is a vital determinant of health and thermal resilience for vulnerable outdoor workers, highlighting how its unequal distribution exacerbates urban health inequities. The shift from “habitual” to “occasional” heat stress reported by traders in these greener areas demonstrates that urban vegetation is not merely an aesthetic amenity but a form of essential infrastructure for thermal resilience.

4.5.2 Street traders-identified mitigation priorities. Stakeholder-derived mitigation strategies overwhelmingly emphasized the need for municipal intervention to provide shade infrastructure (e.g., designated shelters, umbrellas) and ensure access to hydration points. These primary recommendations were augmented by proposals for green infrastructure, such as tree planting, and for expanded preventative health services. Together, these measures form a multi-faceted public health approach to adapting to occupational heat stress. These clinical manifestations show a strong correspondence with remote sensing data documenting elevated land surface temperatures (LST) in Bulawayo’s urban core, particularly the 2022 summer peak of 43.4°C recorded in high-density commercial zones [29,36]. The integration of these physical interventions with proposals for expanded preventative health services is what creates a truly “multi-faceted public health approach.” The high incidence of neurological symptoms (headaches, 98.7%) and the alarming rate of fainting (63.3%) are clear indicators of severe heat strain. As noted by the IPCC [63], such symptoms are precursors to more deadly heatstroke, and their prevalence underscores a failure of existing occupational health protections for informal workers. This finding aligns with the ILO’s [12] concerns about productivity loss and health impacts on vulnerable labour forces in a warming climate.

4.6 Implications for urban planning, public health, and recommendations

The findings of this study support several evidence-based mitigation strategies. Urban greening initiatives in market areas could reduce land surface temperature (LST) by 2–4°C, as demonstrated in comparable settings [62]. Cool roof implementation in commercial districts has shown potential to lower indoor temperatures by 3.7°C. Workplace interventions, such as scheduled shade breaks, have reduced heat illness incidence by 38% in similar contexts, while mobile heat alert systems have proven effective in improving worker protection.

These results demonstrate the critical need for integrated urban climate adaptation strategies in Bulawayo. With LST increasing at a rate of 0.28°C per decade ($p=0.014$) during peak summer months, protecting vulnerable outdoor workers requires combining public health monitoring with targeted cooling interventions [64]. This study establishes a methodological framework for linking community health indicators with urban thermal landscapes, providing a model for climate-health vulnerability assessments in developing cities facing similar challenges of rapid urbanisation and climate change.

The LST analysis in Bulawayo highlights urgent needs for climate-adaptive urban planning and public health interventions in rapidly growing African cities [65]. The study demonstrates that vegetated areas ($NDVI > 0.3$) maintain significantly lower temperatures (3–5°C) than built-up zones, underscoring the critical role of green infrastructure in heat mitigation. Strategic interventions should prioritise expanding urban tree canopies in high-density areas, developing green corridors along transit routes, and implementing cool roofs in commercial districts [46,59].

Thermal disparities between land uses necessitate climate-resilient urban design, including mixed-use development to reduce impervious surfaces, regulations for high-albedo building materials, and water-sensitive urban design in drought-prone areas [54,53]. Public health measures must address vulnerable populations like street traders, who report severe heat-related symptoms (e.g., 98.7% headaches, 63.3% fainting). Recommended actions include heat early-warning systems, shaded rest areas, and occupational health programs [9,66].

Future efforts should integrate localised heat vulnerability mapping using AI-driven microclimate models and community-led cooling initiatives, such as participatory tree-planting and cool pavement pilots [29,36]. Policy integration is essential, requiring climate-responsive building codes and cross-departmental heat governance frameworks. This study provides a blueprint for African cities to combine remote sensing, equitable planning, and public health strategies for climate resilience.

4.7 Limitations and future research directions

This study has several methodological and scope-related limitations. Methodologically, the reliance on Landsat data, despite its long-term availability, may introduce errors due to sensor differences between Landsat 5 TM and Landsat 8 OLI, particularly in thermal band resolutions and atmospheric correction processes. Although robust, the validation of land surface temperature (LST) using SURFRAD stations and water bodies may not fully capture the heterogeneity of urban surfaces in Bulawayo, potentially skewing the results. The survey component, while insightful, is limited by its sample size ($n=150$ street traders) and its reliance on self-reported health symptoms, which may not account for all heat-related impacts or demographic variability. Geographically, the study's exclusive focus on Bulawayo limits the generalisability of the findings to other African cities with different climatic or urban conditions. Additionally, the analysis does not deeply explore socio-economic factors (e.g., income, access to healthcare) that could modulate heat vulnerability among street traders.

Future research should address these gaps by incorporating higher-resolution thermal data (e.g., from Sentinel-3) to improve LST accuracy, expanding validation to include local weather stations, and integrating mixed-methods approaches (e.g., wearable sensors) to objectively measure physiological health impacts. Broader comparative study across multiple cities is necessary to identify regional patterns in urban heat dynamics. Furthermore, investigating the socio-economic determinants of heat vulnerability and empirically testing targeted interventions (e.g., shaded rest areas, cool roofs) would

enhance the development of practical, evidence-based policy recommendations. Finally, longitudinal studies are essential to track the long-term health and productivity effects of rising temperatures on informal workers.

5. Conclusion

This study provides a comprehensive and empirically robust analysis of the intricate nexus between land use change, elevated land surface temperatures (LST), and the resultant health risks for street traders in Bulawayo, Zimbabwe. By integrating multi-temporal remote sensing analysis with detailed socio-economic surveys, the research moves beyond merely characterizing the urban heat island (UHI) effect to explicitly quantify its human cost on a vulnerable, yet essential, segment of the urban workforce.

The geospatial findings unequivocally demonstrate that Bulawayo has undergone significant warming, particularly during the critical summer months of October to December, with minimum night-time temperatures showing a statistically significant increase. This trend is spatially heterogeneous and directly correlated with land cover: built-up zones characterised by a high Dry Built-up Index (DBI) and bare surfaces (high DBSI) exhibit LST 3–5°C higher than vegetated, low-density areas. The radical transformation of the urban landscape—a 228% increase in built-up area since 1984—is a primary driver of this intensified thermal environment, creating a cityscape increasingly dominated by heat-absorbing materials.

Crucially, this thermal disparity is not an abstract climatic phenomenon but a direct determinant of public health. The survey data reveal an alarming prevalence of heat-related morbidity among street traders, with near-universal reports of symptoms like headaches (98.7%), dehydration (84.7%), and profuse sweating (84%). The spatial concordance between MODIS-derived LST hotspots and self-reported symptom clusters provides powerful evidence that traders operating in the CBD, industrial, and high-density residential areas are bearing the brunt of this urban heating. The finding that a majority experience at least five co-occurring symptoms underscores that heat stress manifests not as isolated incidents but as a syndemic of physiological strain, framing extreme heat as a critical occupational health and workers' rights issue.

The stark perceptual contrast reported by traders in vegetated, low-density areas—who experience only occasional symptoms compared to the habitual suffering of those in high-DBI zones—validates urban greenery as essential public health infrastructure. This evidence positions strategies like urban forestry and water-sensitive design not as aesthetic amenities but as non-negotiable components of climate adaptation and equitable urban planning.

Therefore, this study concludes that the effects of land use on surface temperatures in Bulawayo are profound and are directly translating into severe health risks for its street traders. The findings necessitate an urgent, multi-pronged policy response grounded in spatial justice. The study recommends: (1) the targeted integration of green and blue infrastructure in thermal hotspots to mitigate LST; (2) the formal provision of shade structures and hydration points in trading zones; (3) the development of heat early-warning systems tailored to outdoor workers; and (4) the reform of urban planning policies to mandate cool materials and preserve green spaces. Ultimately, protecting the health and economic resilience of the informal workforce is integral to building sustainable, liveable, and climate-resilient cities in the Global South. This research establishes a replicable framework for integrating geospatial science with public health assessment, providing a vital blueprint for urban authorities seeking to safeguard their most vulnerable populations from the escalating threats of urban heating.

Supporting information

S1 Table. Street traders responses Excel sheet.

(XLSX)

S1 Text. Extracting LSTs files.

(DOCX)

Author contributions

Conceptualization: Shelton Mthunzi Sithole, Walter Musakwa, James Magidi.

Data curation: Shelton Mthunzi Sithole.

Formal analysis: Shelton Mthunzi Sithole, Walter Musakwa.

Investigation: Shelton Mthunzi Sithole, Walter Musakwa, James Magidi.

Methodology: Shelton Mthunzi Sithole, Walter Musakwa, James Magidi.

Project administration: Shelton Mthunzi Sithole.

Resources: Shelton Mthunzi Sithole.

Software: Shelton Mthunzi Sithole.

Supervision: Shelton Mthunzi Sithole, Walter Musakwa, James Magidi.

Validation: Shelton Mthunzi Sithole, James Magidi.

Visualization: Shelton Mthunzi Sithole.

Writing – original draft: Shelton Mthunzi Sithole.

Writing – review & editing: Shelton Mthunzi Sithole, Walter Musakwa, James Magidi.

References

1. Moore M, Gould P, Keary BS. Global urbanization and impact on health. *Int J Hyg Environ Health*. 2003;206(4–5):269–78. <https://doi.org/10.1078/1438-4639-00223> PMID: 12971682
2. Faqe Ibrahim G. Urban land use land cover changes and their effect on land surface temperature: case study using Dohuk City in the Kurdistan Region of Iraq. *Climate*. 2017;5(1):13. <https://doi.org/10.3390/cli5010013>
3. Odindi JO, Nongebeza S, Siro N. The influence of seasonal land-use-land-cover transformation on thermal characteristics within the city of Pietermaritzburg. *SA J of Geomatics*. 2022;9(2):348–64. <https://doi.org/10.4314/sajg.v9i2.23>
4. Tabassum A, Basak R, Shao W, Haque MM, Chowdhury TA, Dey H. Exploring the Relationship Between Land Use Land Cover and Land Surface Temperature: a Case Study in Bangladesh and the Policy Implications for the Global South. *J geovis spat anal*. 2023;7(2). <https://doi.org/10.1007/s41651-023-00155-z>
5. Li X, Stringer LC, Chapman S, Dallimer M. How urbanisation alters the intensity of the urban heat island in a tropical African city. *PLoS One*. 2021;16(7):e0254371. <https://doi.org/10.1371/journal.pone.0254371> PMID: 34255779
6. Avashia V, Garg A, Dholakia H. Understanding temperature related health risk in context of urban land use changes. *Landscape and Urban Planning*. 2021;212:104107. <https://doi.org/10.1016/j.landurbplan.2021.104107>
7. Gyimah RR, Kwang C, Antwi RA, Morgan Attua E, Owusu AB, Doe EK. Trading greens for heated surfaces: Land surface temperature and perceived health risk in Greater Accra Metropolitan Area, Ghana. *The Egyptian Journal of Remote Sensing and Space Sciences*. 2023;26(4):861–80. <https://doi.org/10.1016/j.ejrs.2023.09.004>
8. Ebi KL, Åström C, Boyer CJ, Harrington LJ, Hess JJ, Honda Y, et al. Using detection and attribution to quantify how climate change is affecting health: Study explores detection and attribution to examine how climate change is affecting health. *Health Affairs*. 2020;39(12):2168–74. <https://doi.org/10.1377/hlthaff.2020.00863>
9. Wright CY, Kapwata T. An urgent call to address climate change-related human health impacts in Southern Africa. *PLOS Clim*. 2023;2(5):e0000204. <https://doi.org/10.1371/journal.pclm.0000204>
10. Lüthi S, Fairless C, Fischer EM, Scovronick N, Ben Armstrong, Coelho MDSZS, et al. Rapid increase in the risk of heat-related mortality. *Nat Commun*. 2023;14(1):4894. <https://doi.org/10.1038/s41467-023-40599-x> PMID: 37620329
11. Working on a warmer planet: The impact of heat stress on labour productivity and decent work International Labour Office – Geneva, ILO, 2019 Available at https://www.ilo.org/sites/default/files/wcmsp5/groups/public/@dgreports/@dcomm/@publ/documents/publication/wcms_711919.pdf
12. ILO I. Working on a warmer planet: the impact of heat stress on labour productivity and decent work. Geneva: International Labour Organization. 2019.
13. Ndossi M, Avdan U. Inversion of Land Surface Temperature (LST) Using Terra ASTER Data: A Comparison of Three Algorithms. *Remote Sensing*. 2016;8(12):993. <https://doi.org/10.3390/rs8120993>
14. Feyissa N. Climate Change Trends, Projections and Vulnerability Integration (Doctoral dissertation, Addis Ababa University Addis Ababa, Ethiopia).

15. Fineberg M. Climate change impacts on Africa's economic growth-Report.2018
16. Asongu SA, Messono OO, Guttemberg KTJ. Women political empowerment and vulnerability to climate change: evidence from 169 countries. *Climatic Change*. 2022;174(3–4). <https://doi.org/10.1007/s10584-022-03451-7>
17. Klöck C, Nunn PD. Adaptation to Climate Change in Small Island Developing States: A Systematic Literature Review of Academic Research. *The Journal of Environment & Development*. 2019;28(2):196–218. <https://doi.org/10.1177/1070496519835895>
18. Sarkodie SA, Strezov V. Economic, social and governance adaptation readiness for mitigation of climate change vulnerability: evidence from 192 countries. *Science of the Total Environment*. 2019;656:150–64.
19. Zhao M, Huang X, Kjellstrom T, Lee JK, Otto M, Zhang X, et al. Labour productivity and economic impacts of carbon mitigation: a modelling study and benefit–cost analysis. *The Lancet Planetary Health*. 2022;6(12):e941-8.
20. Sithole SM, Musakwa W, Magidi J, Kibangou AY. Characterising landcover changes and urban sprawl using geo-spatial techniques and landscape metrics in Bulawayo, Zimbabwe (1984–2022). *Heliyon*. 2024.
21. Mpfou B. Perpetual 'Outcasts'? Squatters in peri-urban Bulawayo, Zimbabwe. *AF*. 2012;25(2). <https://doi.org/10.21825/af.v25i2.4946>
22. Mokarram M, Taripanah F, Pham TM. Investigating the effect of surface urban heat island on the trend of temperature changes. *Advances in Space Research*. 2023;72(8):3150–69. <https://doi.org/10.1016/j.asr.2023.06.048>
23. Kjellstrom T, Briggs D, Freyberg C, Lemke B, Otto M, Hyatt O. Heat, Human Performance, and Occupational Health: A Key Issue for the Assessment of Global Climate Change Impacts. *Annu Rev Public Health*. 2016;37:97–112. <https://doi.org/10.1146/annurev-publhealth-032315-021740> PMID: [26989826](https://pubmed.ncbi.nlm.nih.gov/26989826/)
24. Sepadi MM. Impact of climate change on informal street vendors: A systematic review to help South Africa and other nations (2015–2024). *Atmosphere*. 2025;16(2):179.
25. Ünsal Ö, Lotfata A, Avci S. Exploring the relationships between land surface temperature and its influencing determinants using local spatial modeling. *Sustainability*. 2023;15(15):11594. <https://doi.org/10.3390/su151511594>
26. ElGendawy A. Integrating planning and climatology for more liveable and heat-resilient cities. Macquarie University.
27. Fu Q, Zheng Z, Sarker MN, Lv Y. Combating urban heat: systematic review of urban resilience and adaptation strategies. *Heliyon*. 2024.
28. Mbira L. The de-industrialisation of Bulawayo manufacturing sector in Zimbabwe: Is the capital vacuum to blame. *International Journal of Economics, Commerce and Management*. 2015;3(3):1–5.
29. Mushore TD, Mutanga O, Odindi J. Understanding growth-induced trends in local climate zones, land surface temperature, and extreme temperature events in a rapidly growing city: a case of Bulawayo Metropolitan City in Zimbabwe. *Front Environ Sci*. 2022;10. <https://doi.org/10.3389/fenvs.2022.910816>
30. Moyo PL, Nunu WN. Oral pre-exposure prophylaxis accessibility, knowledge, barriers, and facilitators among men who have sex with men in Bulawayo, Zimbabwe. *Am J Mens Health*. 2023;17(5). <https://doi.org/10.1177/15579883231207481> PMID: [37876122](https://pubmed.ncbi.nlm.nih.gov/37876122/)
31. Mukuhlani T, Nyamupingidza MT. Water scarcity in communities, coping strategies and mitigation measures: the case of Bulawayo. *JSD*. 2014;7(1). <https://doi.org/10.5539/jsd.v7n1p144>
32. He T, Guo J, Xiao W, Xu S, Chen H. A novel method for identification of disturbance from surface coal mining using all available Landsat data in the GEE platform. *ISPRS Journal of Photogrammetry and Remote Sensing*. 2023;205:17–33. <https://doi.org/10.1016/j.isprsjprs.2023.09.026>
33. Ermida SL, Soares P, Mantas V, Götsche F-M, Trigo IF. Google earth engine open-source code for land surface temperature estimation from the landsat series. *Remote Sensing*. 2020;12(9):1471. <https://doi.org/10.3390/rs12091471>
34. Vanhellefont Q. Adaptation of the dark spectrum fitting atmospheric correction for aquatic applications of the Landsat and Sentinel-2 archives. *Remote Sensing of Environment*. 2019;225:175–92. <https://doi.org/10.1016/j.rse.2019.03.010>
35. Zhang T, Zhou Y, Zhu Z, Li X, Asrar GR. A global seamless 1 km resolution daily land surface temperature dataset (2003–2020). *Earth System Science Data Discussions*. 2021;2021:1–6.
36. Mushore TD, Mutanga O, Odindi J, Sadza V, Dube T. Pansharpened landsat 8 thermal-infrared data for improved Land Surface Temperature characterization in a heterogeneous urban landscape. *Remote Sensing Applications: Society and Environment*. 2022;26:100728. <https://doi.org/10.1016/j.rsase.2022.100728>
37. Yue W, Xu J, Tan W, Xu L. The relationship between land surface temperature and NDVI with remote sensing: application to Shanghai Landsat 7 ETM+ data. *International Journal of Remote Sensing*. 2007;28(15):3205–26. <https://doi.org/10.1080/01431160500306906>
38. Begum MS, Bala SK, Islam AS, Islam GT, Roy D. An analysis of spatio-temporal trends of land surface temperature in the Dhaka Metropolitan Area by Applying Landsat Images. *JGIS*. 2021;13(04):538–60. <https://doi.org/10.4236/jgis.2021.134030>
39. Yin CL, Meng F, Yu QR. Calculation of land surface emissivity and retrieval of land surface temperature based on a spectral mixing model. *Infrared Physics & Technology*. 2020;108:103333. <https://doi.org/10.1016/j.infrared.2020.103333>
40. Diaz LR, Santos DC, Käfer PS, Rocha NS, Costa ST, Kaiser EA, et al. Atmospheric correction of thermal infrared Landsat images using high-resolution vertical profiles simulated by WRF model. *Environmental Sciences Proceedings*. 2021;8(1):27.
41. Change IP. Climate change 2007: Impacts, adaptation and vulnerability. Geneva, Suíça. 2001.

42. Parastatidis D, Mitraka Z, Chrysoulakis N, Abrams M. Online Global Land Surface Temperature Estimation from Landsat. *Remote Sensing*. 2017;9(12):1208. <https://doi.org/10.3390/rs9121208>
43. Gandotra A. Street vending: A successive sector of urban informal economy. *Indian JL & Legal Rsch*. 2023;5(1):1.
44. Raji T, Wamalwa F, Williams NJ. Dual perspectives: a remote sensing- and survey-based exploration of the determinants of irrigation use in Northern Ethiopia. *Environ Res: Food Syst*. 2025;2(2):025003. <https://doi.org/10.1088/2976-601x/adb84f>
45. Zhou B, Rybski D, Kropp JP. The role of city size and urban form in the surface urban heat island. *Sci Rep*. 2017;7(1):4791. <https://doi.org/10.1038/s41598-017-04242-2> PMID: 28684850
46. Schwaab J, Meier R, Mussetti G, Seneviratne S, Bürgi C, Davin EL. The role of urban trees in reducing land surface temperatures in European cities. *Nat Commun*. 2021;12(1):6763. <https://doi.org/10.1038/s41467-021-26768-w> PMID: 34815395
47. Twomey D, Petrass L, Harvey J, Otago L, LeRossignol P. Heat experienced on synthetic turf surfaces: An inevitable or preventable risk?. *Journal of Science and Medicine in Sport*. 2014;e119-20.
48. van Huijgevoort MHJ, Cirkel DG, Voeten JGWF. Climate adaptive solution for artificial turf in cities: integrated rainwater storage and evaporative cooling. *Front Sustain Cities*. 2024;6. <https://doi.org/10.3389/frsc.2024.1399858>
49. Akinyemi FO, Ikanyeng M, Muro J. Land cover change effects on land surface temperature trends in an African urbanizing dryland region. *City and Environment Interactions*. 2019;4:100029. <https://doi.org/10.1016/j.cacint.2020.100029>
50. Hua AK, Ping OW. The influence of land-use/land-cover changes on land surface temperature: a case study of Kuala Lumpur metropolitan city. *European Journal of Remote Sensing*. 2018;51(1):1049–69. <https://doi.org/10.1080/22797254.2018.1542976>
51. Roffe SJ, van der Walt AJ, Fitchett JM. Spatiotemporal characteristics of human thermal comfort across southern Africa: An analysis of the Universal Thermal Climate Index for 1971–2021. *Intl Journal of Climatology*. 2023;43(6):2930–52. <https://doi.org/10.1002/joc.8009>
52. Herring SC, Hoell A, Hoerling MP, Kossin JP, Schreck CJ, Stott PA. Explaining Extreme Events of 2015 from a Climate Perspective. *Bulletin of the American Meteorological Society*. 2016;97(12):S1–145. <https://doi.org/10.1175/bams-explainingextremeevents2015.1>
53. Mpendeli S, Nhamo L, Moeletsi M, Masupha T, Magidi J, Tshikolomo K, et al. Assessing climate change and adaptive capacity at local scale using observed and remotely sensed data. *Weather and Climate Extremes*. 2019;26:100240. <https://doi.org/10.1016/j.wace.2019.100240>
54. Estoqu e RC, Ooba M, Togawa T, Hijioka Y, Murayama Y. Monitoring global land-use efficiency in the context of the UN 2030 Agenda for Sustainable Development. *Habitat International*. 2021;115:102403.
55. Lee H, Calvin K, Dasgupta D, Krinmer G, Mukherji A, Thorne P, et al. Synthesis report of the IPCC Sixth Assessment Report (AR6), Longer report. IPCC.
56. OKE T. The energetic basic of the urban heat island. *Quarterly Journal of the Royal Meteorological Society*. 1982;108(455):1–24. <https://doi.org/10.1256/smsqj.45501>
57. Yaşlı R, Yücedağ C, Ayan S, Simovski B. The role of urban trees in reducing land surface temperature. *SilvaWorld*. 2023;2(1):36–49.
58. Wang W, Teng H, Zhao L, Han L. Long-Term changes in water body area dynamic and driving factors in the middle-lower Yangtze Plain based on multi-source remote sensing data. *Remote Sensing*. 2023;15(7):1816. <https://doi.org/10.3390/rs15071816>
59. Bowler DE, Buyung-Ali L, Knight TM, Pullin AS. Urban greening to cool towns and cities: A systematic review of the empirical evidence. *Landscape and Urban Planning*. 2010;97(3):147–55. <https://doi.org/10.1016/j.landurbplan.2010.05.006>
60. Kumar V. Climate Change Impacts on Human Health. *Current Research in Medical Sciences*. 2024;3(1):1–9.
61. Ali MI, Hasim AH, Abidin MR. Monitoring the built-up area transformation using urban index and normalised difference built-up index analysis. *International Journal of Engineering Transactions B: Applications*. 2019;32(5):647–53.
62. Magidi J, Ahmed F. Assessing urban sprawl using remote sensing and landscape metrics: A case study of City of Tshwane, South Africa (1984–2015). *The Egyptian Journal of Remote Sensing and Space Science*. 2019;22(3):335–46.
63. IPCC (Intergovernmental Panel on Climate Change). Global Warming of 1.5° C. An IPCC Special Report on the impacts of global warming of 1.5° C above pre-industrial levels and related global greenhouse gas emission pathways in the context of strengthening the global response to the threat of climate change, sustainable development, and efforts to eradicate poverty. Geneva: IPCC; 2018 Dec.
64. Kunda JJ, Gosling SN, Foody GM. The effects of extreme heat on human health in tropical Africa. *Int J Biometeorol*. 2024;68(6):1015–33. <https://doi.org/10.1007/s00484-024-02650-4> PMID: 38526600
65. Scholes R, Engelbrecht F. Climate impacts in southern Africa during the 21st century. Global Change Institute, University of Witwatersrand. 2021.
66. Harlan SL, Ruddell DM. Climate change and health in cities: impacts of heat and air pollution and potential co-benefits from mitigation and adaptation. *Current Opinion in Environmental Sustainability*. 2011;3(3):126–34. <https://doi.org/10.1016/j.cosust.2011.01.001>